THE PHYSICAL AND METALLURGICAL ASPECTS OF HYDROGEN IN METALS

R.A. Oriani
Department of Chemical Engineering and Materials Science
The University of Minnesota
Minneapolis, MN 55455

Abstract

To attempt to optimize the anomalous phenomena that today go under the label "cold fusion" the experimentalist should be aware of the many aspects of the behavior of hydrogen in metals and of its entry into and egress from metals. This paper discusses the equilibrium characteristics of the isotopes of hydrogen in metals. The first section discusses the thermodynamics of the terminal solutions of metal-hydrogen systems including the enthalpies of solutions, H-H interactions, effect of third elements, distribution of isotopes between the phases, site occupation, and the molar volume of hydrogen in metallic solutions.

The mobility of hydrogen in a metal lattice is a very large subject. This discussion is restricted to the kinetics of hydrogen diffusion, at and above room temperature, with respect to the variation with temperature, hydrogen concentration, isotopic mass and concentration of third elements. A distinction is made between the effects on the mobility and the effects associated with the non-ideality of the solution. The decrease of the diffusivity due to attractive interactions with lattice defects such as those generated by cold work are discussed in terms of trapping theory. Brief consideration is given to diffusion of hydrogen along grain boundaries and along dislocation cores as well as to diffusion motivated by gradients of electrical potential, of temperature and of mechanical stress.

When hydrogen is absorbed from the molecular gas at fixed pressure and temperature, the overall driving force can be expressed in terms of thermodynamic parameters; the kinetic impediments to the ingress of hydrogen control the rate of entry and these are discussed. When hydrogen is presented to the metal by electrochemical means or by partially dissociated hydrogen gas the driving force for entry into the metal cannot be expressed thermodynamically, although the concept of input fugacity is often used. This concept is discussed and incorrect inferences sometimes made from it are pointed out. The entry and the egress of hydrogen produces mechanical stresses in the metal which modify the thermodynamics of metal-hydrogen systems. They necessitate a distinction to be made between coherent and incoherent phase diagrams, and change the driving force for the exchange of hydrogen between the metal and the environing gas phase. More importantly, the generated stresses can relax by producing

dislocations, grain rotation, cracks and microvoids. Examples of these phenomena are discussed. The generation of such lattice defects interacts in complicated ways with the intrinsic decohesioning effect of dissolved hydrogen to seriously affect the mechanical properties of metals. Some implications of these considerations for cold fusion research are pointed out.

Introduction

In a field like cold fusion in which experimental results are very difficult to reproduce it is beneficial to understand as well as possible the materials used in the experiments and the processes and reactions to which they are subjected. The phenomena accompanying the input of hydrogen into metals and the behavior of hydrogen therein have been investigated to a considerable extent for metals of construction. It appears useful to review that body of information and to show its relevance to metals of interest to cold fusion.

The paper first briefly discusses some equilibrium phenomena for hydrogen in metals that are useful for understanding the subsequent topics. In this section particular attention is given to the generation and the relaxation of mechanical stresses. The second section deals with the mobility of hydrogen within and upon the metal, as affected by lattice imperfections and as driven by various forces. The entry of hydrogen into the metal is considered in the third section with particular attention to the accompanying stress generation and its relaxation by dislocation generation and motion. The concomitant changes of shape and of surface topography are presented and discussed. The concept of input fugacity, which has led to some misconceptions in the past, is explained. The next short section very briefly touches on the manner in which hydrogen affects the mechanical properties of metals. The final section presents some of the implications of the foregoing material for cold fusion research.

For further information on some of the topics touched on in this review the reader is referred the books edited by Alefeld and Volkl (1), Kirchheim et al. (2).

Equilibrium Aspects of Hydrogen in Transition Metals

The Dissociated State of Dissolved Hydrogen

At moderate pressures, the concentration of hydrogen dissolved in solid metals is described to a good approximation by the empirical relation known as Sievert's law

$$c = sp^{1/2} \qquad (1)$$

where c is the concentration of dissolved hydrogen in equilibrium with gaseous hydrogen at pressure p, and s is the Sievert's parameter. If the equilibrium between gaseous hydrogen and dissolved hydrogen $\underline{H}$, is assumed to be

$$\frac{1}{2}H_2(g) = \underline{H} \qquad (2)$$

then one can write

$$a = Kf^{1/2} \qquad (3)$$

where a is the thermodynamic activity of the dissolved hydrogen, $\underline{H}$, f is the fugacity of the gaseous hydrogen, and K is the equilibrium constant for reaction (2). The activity

$$a = \gamma c \qquad (4)$$

at low concentrations where γ is an activity coefficient which at low concentrations is independent of c, and similarly, at low pressures $f = \beta p$, in which β is a fugacity coefficient which at low p is essentially unity. Hence, (1) can be written as

$$c = (K/\gamma\beta^{1/2})p^{1/2} \qquad (5)$$

so that $s = K/\gamma\beta^{1/2} \approx$ constant at a given temperature and over a small concentration range. The experimental verification of Sievert's law for a gas-metal system proves that the molecular gas dissociates upon dissolution in the metal. Furthermore, recalling that $\ln K = -\Delta\overline{G}^\circ/RT$, where ΔG° is the change of Gibbs free energy between standard states for reaction (2), one obtains

$$\ln s = -\Delta\overline{G}^\circ/RT - \ln(\gamma\beta^{1/2})$$

$$= -\frac{\Delta\overline{H}^\circ}{RT} + \frac{\Delta\overline{S}^\circ}{R} - \ln(\gamma\beta^{1/2}) \qquad (6)$$

In eq. (6), $\Delta\overline{H}^\circ$ and $\Delta\overline{S}^\circ$ are, respectively, the partial molal enthalpy and the entropy changes between standard states for reaction (2).

The partial molal enthalpy of solution, $\Delta\overline{H}^\circ$, maybe positive or negative, and metals are conventionally divided into endothermic and exothermic absorbers of hydrogen. There is no fundamental significance in this classification as to the qualitative aspects of the electronic interaction between $\underline{H}$ and the metal. It only categorizes metals into the group for which the energy of electronic interaction with dissolved hydrogen is a smaller, but negative quantity, than the energy of dissociation of molecular hydrogen, and into the class for which the opposite is the case. The important phenomenological distinction between the groups is that metals for which $\Delta\overline{H}^\circ < 0$ display a concentration (solubility) decreasing with increasing temperature, and those for which $\Delta\overline{H}^\circ > 0$ have the opposite behavior. As the concentration of dissolved hydrogen is increased, the activity coefficient of the dissolved hydrogen varies because of interactions between the hydrogens and because the electronic interaction between the hydrogen and the host

metal varies with concentration. This is reflected in the composition dependence of the quantities $\Delta\overline{H} = \overline{H} - \overline{H}°$ and $\Delta\overline{S} = \overline{S} - \overline{S}°$ for the dissolved hydrogen. As c increases a hydrogen-containing phase other than the terminal solid solution usually develops. This topic will be considered in a subsequent section.

The $\Delta\overline{G}°$ values, and hence the equilibrium constants, K, for reaction (2) are functions not only of temperature but also of the isotopic mass of hydrogen. For example, for the palladium-hydrogen* system

$$\ln K_H = \frac{1163}{T} - 6.45$$

and

$$\ln K_D = \frac{949}{T} - 6.40$$

in which the temperature T is in degrees Kelvin (3). Also, according to (4), for tritium, T,

$$\ln K_T = \frac{832}{T} - 6.25.$$

Consequently, for the same concentration and temperature, deuterium (D) and tritium (T) have higher equilibrium pressures in Pd than does protium (H). If one defines the equilibrium distribution of the isotopes H and D between the palladium (Pd) and the gas phase (g) as (n_i = number of i atoms):

$$\alpha^{g}_{Pd}(D,H) = \frac{(n_D / n_H)_g}{(n_D / n_H)_{Pd}} = \frac{(2p_{O_2} + p_{HD}) / (2p_{H_2} + p_{HD})}{(n_D / n_H)_{Pd}},$$

the measurements of Clewley et al. (5) yield, as the average of measurements on β-phase Pd(H),

$$\ln \alpha^{g}_{Pd}(D,H) = \frac{178}{T} + 0.175 = 2.16 \text{ at } 298 \text{ K}.$$

The equilibrium separation factor for tritium and protium in Pd was measured by Sicking (6) as

$$\ln \alpha^{g}_{Pd}(T,H) = \frac{320}{T} - 0.075 = 2.71 \text{ at } 298 \text{ K}.$$

* In this review, the term "hydrogen" is usually employed generically to signify all of the isotopes of hydrogen. However, in some portions where isotopic differences are discussed, "hydrogen" refers to protium, the lightest isotope.

The equilibrium separation factor for two isotopes between liquid water, L, and palladium can be defined as $\alpha^{L}_{Pd}(D,H) = (n_D/n_H)_L / (n_D/n_H)Pd$. Sicking (7) measured $\alpha^{L}_{Pd}(D,H) = 9.0$ at 298 K, and $\alpha_{Pd}(T,H)$ has been estimated (8) as 12.0 at 298 K. Note that the equilibrium distribution is different from the kinetically determined separation factors for cathodic deposition. For H and D on Pd-Pg alloy, the electrolytic separation factor, $\alpha = 9$ to 16 (9). See also ref. (10). Thus, in the case of palladium, the heavier isotope is favored in the gas phase.

At 298K and 1 bar of hydrogen pressure, $n_D/n_{Pd} = 0.65$ and $n_H/n_{Pd} = 0.7$. Similarly, deuterium adsorbed on Pd has a larger equilibrium pressure than does protium adsorbed on Pd at comparable coverage (11). However, Pd must be considered anomalous since other metals since other metals exhibit the opposite behavior; deuterium dissolved in Ta, Nb, or V exhibits smaller equilibrium pressures than does protium dissolved in these metals at the same concentrations and temperatures (8).

Interstitial Site Occupancy

Because the volume of a hydrogen atom, on a molar basis, is about 0.3 cm^3/mol, much smaller than the molar volume of a transition metal, the observed expansion of a metal lattice upon dissolution of hydrogen is evidence that the solution is not substitutional. That hydrogen occupies interstitial positions in metal lattices has been demonstrated by neutron diffraction in several cases and inferred from other evidence in other cases (1). The face-centered cubic lattice has one octahedral interstitial site per metal atom (at 1/2, 0, 0 and equivalent positions), and two tetrahedral interstitial sites per metal atom (at 1/4, 1/4, 1/4 and equivalent positions). The body-centered cubic lattice has three octahedral interstitial sites per metal atom (at the centers of the cube faces and of the cube edges) and six tetrahedral interstitial sites per metal atom (at 1/2, 1/4, 0) and equivalent positions). In the f.c.c. lattice the octahedral positions have the larger free volume, whereas in the b.c.c. lattice the tetrahedral sites are the larger.

Table 1 collects information on the location of dissolved hydrogen in various metals, and the magnitudes of the partial molal volumes, $\bar{V}$, of the dissolved hydrogen, where $\bar{V} = (\partial V/\partial m)$ at constant number of metal atoms, temperature, and pressure; V is the volume of the metallic solution and m is the number of moles of hydrogen introduced into the metallic system. Introduction of a hydrogen atom into an interstitial position increases the volume of the system by about 1/5 of the amount of the volume increase caused by the addition of one metal atom.

The displacement of the metal atoms by the introduction of a hydrogen atom can be represented (13) by virtual forces (the Kanzaki forces) applied to each lattice atom to reproduce the actual displacement of the metal atom. The Kanzaki force distribution is describable by a multipole expansion of which the dipole term, P_{ij} is usually sufficient, where

$$P_{ij} = \sum_m f_j^m x_i^m$$

with f_i^m being the Kanzaki force applied to the m'th atom situated at the distance x^m from the hydrogen atom. Because the octahedral sites of the f.c.c. lattice provide six metal atoms equidistant from the occupying hydrogen atom, P_{ij} is isotropic. However, around the octahedral site of the b.c.c. lattice two metal atoms are farther than the other four from the occupying solute atom so that the dipolar character of the force distribution, and the orientation of the dipole must in general be taken into account. In the case of interstitial carbon atoms in b.c.c. iron, the dipolar distortion is important and is responsible for the Snoek effect (13). In any case, for a random distribution of n_H hydrogen atoms in interstitial sites in a metal of atomic volume Ω, the volume change due to the hydrogens as measured by the change of lattice parameter, a, is

$$3\frac{\Delta a}{a} = \frac{\Delta V}{V} = (n_H/3\Omega)\kappa \text{Trace } P_{ij},$$

where κ is the compressibility.

To obtain an intuitive feel for the stress state produced by the occupation of an interstitial site by hydrogen (or other solute) it is useful to consider the "ball-in-hole" model in continuum elasticity (29). Consider an incompressible sphere (simulating the solute atom) fitted into a spherical cavity in a matrix (the cavity simulates the interstitial site), the cavity being smaller than the ball. If ΔV_1 is the volume change of the cavity occasioned by forcing in the incompressible ball, the outer free surface of the matrix will sweep over an additional volume (29)

$$\Delta V_2 = \frac{3(1-\nu)}{1+\nu}\Delta V_1$$

where ν is the Poisson ratio of the matrix. For a typical value of ν of 0.3, ΔV_2 is larger than ΔV_1 by 50%. This result is a consequence of the boundary condition that the outer surface of the matrix be stress free. Thus, the volume of the body increases by an amount larger than that required to accommodate the solute atom; this is the origin of the increase in lattice parameter produced in a metal lattice upon a absorption of hydrogen. It should be noted that whereas the misfitting ball is under compression by the expanded matrix, the matrix has zero hydrostatic component of stress and its external surface has zero stress. The argument is not changed when more than one center of dilatation is considered. A homogeneous distribution of interstitial solutes produces a matrix in which the interstitial sites are larger than in the solute-free matrix. It follows that the partial molal volume of an interstitial solute should decrease with increasing concentration (8). It is worth noting at this point that although equal concentrations of hydrogen may be injected into a metal by equilibrating with high-pressure molecular gas or by subjecting the metal to cathodic charging, the internal thermodynamic state of the dissolved hydrogen will be different in these two conditions. The large gas pressure upon the metal in the first case will decrease the expanding effect of the interstitial hydrogen by compressing the metal, whereas in the second case because of the absence of pressure on the external surface of the metal there will not be any decrease of the intrinsic expanding effect.

The occupation by hydrogen of interstitial sites, which necessarily constitute a finite population in any one specimen, leads to a thermodynamic description of the dissolved hydrogen in terms of Fermi-Dirac statistics. Thus, the activity of the dissolved hydrogen must be expressed more generally than by eq. (4) as

$$\mu = \mu^o + RT\ln a = \mu^o + RT \ln\left(\frac{\gamma\theta_1}{1-\theta_1}\right) \qquad (7)$$

Here, $\theta_1 = n_H/n_{s1}$, where n_H is the number of dissolved hydrogen atoms and n_{s1} is the number of interstitial positions of the class that produce the lowest Gibbs free energy state. In palladium s_1 would represent the octahedral positions. The important consequence of this is that as $\theta_1 \rightarrow 1$ the chemical potential, μ, of the interstitial hydrogen rises to very large values. Indeed, the source of the hydrogen cannot have a sufficiently high chemical potential to cause the filling of all of the lowest-energy class of sites. Therefore, a sufficiently large μg^{as} would cause the next-higher energy class of interstitial sites to become partially populated at $\theta_1 < 1$. In the case of palladium one would predict some tetrahedral site occupancy at θ_1 (octahedral) < 1. Although data appear not to be available to verify this assertion about palladium, neutron diffraction (30) on V(D) at $n_D/n_V = 0.5$ showed that about 90% of the dissolved deuterium atoms occupy tetrahedral sites in the b.c.c. lattice, the rest being on octahedral positions. Similar results were found by Chervyakov et al. (31) with $n_D/n_V = 0.8$ in which 7% of the deuterium atoms are located on octahedral sites. It is also possible that interactions between the dissolved hydrogen atoms cause energetic distinctions between subclasses of interstitial sites of one symmetry type. Taking only one example, in the Ta (H) phase about the composition $n_H/n_{Ta} = 1/2$, the hydrogens occupy tetrahedral sites on only alternate $(\bar{1}10)$ planes (32,33), which of course means that the H atoms form an ordered sublattice. Hydrogen atoms in excess of $n_H/n_{Ta} = 1/2$ are accommodated in tetrahedral sites in the adjacent $(\bar{1}10)$ planes.

Hydrogen-Metal Interactions

The enthalpy of solution of hydrogen from the molecular gas into the metal is composed of two terms: the energy of dissociation of the molecule, which is, of course, independent of the nature of the metal, and the energy of interaction between the dissolved hydrogen atoms, and between the hydrogen and the metal. The latter term varies much from metal to metal and this variation is responsible for the phenomenological separation of metals into the two classes of endothermic and exothermic "occluders" of hydrogen. The latter term has been much investigated, especially for palladium, and presents challenging theoretical difficulties. The interests of the intended audience or this paper are served by a description of the broad picture for hydrogen in the transition metals.

Because measurements of physical properties such as the electronic specific heat, the magnetic susceptibility, the electrical resistance, the thermoelectric power, photoemission, etc., show much larger variation with hydrogen concentration than can

be attributed simply to the lattice expansion caused by hydrogen, it is clear that hydrogen strongly perturbs the electronic structure of the host metals. Although details differ from one metal to another, the broad picture is that the 1s- electron that accompanies the hydrogen nucleus enters the s- and d- bands of the host metal changing the density of states at the Fermi surface and causing shifts of the energy bands. The Fermi electrons then concentrate around the positive hydrogen nucleus to produce a closely screened entity that may loosely be thought of as a neutral atom, although the screening electrons are not in bound states.

Because the electron energy bands are affected there are long-range interactions between the dissolved hydrogens, and because of the localized heaping up of Fermi electrons about the hydrogen nuclei there are also short-range interactions among the hydrogens. Fritsche et al. (34) adduce repulsive interactions between the two hydrogens for the d-holes in the electronic structure of the Pd atom that is the common neighbor to both hydrogens. On the other hand, the hypothesis of attractive interactions between adjacent hydrogens produces a good description of the thermodynamic properties of Pd(H) solutions (8). The attractive interaction has been ascribed to the oscillatory decay of Fermi electron density about the hydrogen nucleus (35) (the so-called "Friedel wiggles"), and to elastic intereactions (36). Attractive interactions between nearest-neighbor hydrogens are consistent with internal friction experiments on Pd(H) (37) which are interpreted as reorientation of H-H pairs, and also with the evidence of hydrogen cluster formation in Pd(H) obtained by inelastic neutron scattering (38). Similarly, long-range interactions between hydrogens and also between hydrogen and other solutes in a metal lattice have been discussed in terms of electronic and elastic interactions. Concentrations of Ag, Sn, Au, B, and Pb increase the concentration of H in palladium for a given hydrogen gas pressure and temperature. This effect is attributed (8) to the expansion of the interstitial sites caused by these solutes (the lattice parameter is increased) so that it costs less energy to place hydrogens in the enlarged sites. However, the solubility enhancement by these solutes occurs only at low hydrogen contents. At larger hydrogen levels these solutes decrease the hydrogen solubility because the metal solutes fill up some of the empty 4d states of the palladium so that fewer electrons coming in with the hydrogen nuclei can be accommodated by the 4d-holes (8). Rh and Ni contract the Pd lattice so that they reduce hydrogen solubility at low hydrogen levels. Rh increases the number of empty 4d states available to hydrogen, so that the solubility of hydrogen is increased at high hydrogen levels.

Since hydrogen changes the local and the global electronic structure of the metal in which it resides, as well as increasing the mean separation between the atoms of the host metal, it is not surprising to find that the cohesive force (the force needed to increase the interatomic distance) between the metal atoms is affected by hydrogen. As yet, no experiment has been devised to measure this effect, but several different theoretical approaches agree that hydrogen reduces the cohesive forces in transition metals. A molecular-dynamics study (39) of Pd(H) has demonstrated that hydrogen reduces the bond strength between Pd atoms by filling antibonding states in the 4d band. Cluster calculations (40) and the embedded atom method (41) have verified that

hydrogen reduces cohesion in several transition metals. McMullen et al. (42) used an effective-medium model to calculate the force required to rigidly separate two halves of a 3d-metal crystal, and have shown that hydrogen decreases the necessary forces for Ti, V, Mn, Fe, Cu, and Ni among others. Fritsche and Muller (43) have demonstrated by cluster calculations that hydrogen weakens Pd-Pd bonds by decreasing the electron density between the metal atoms.

Interactions of Hydrogen with Lattice Imperfections

Metal lattices exhibit structural defects of various dimensionalities. "Zero-dimensional" defects are vacancies and self-interstitials of which the former can have concentrations consistent with thermodynamic equilibrium, increasing with increasing temperature. Both defects can be generated by plastic deformation and vacancies can be quenched in from high temperatures to produce populations in excess of the equilibrium value. Data for the interaction between these defects and dissolved hydrogen are scarce. Kirchheim (44) found that at concentrations of hydrogen in Pd below 40 ppm, the partial molal volume of hydrogen is a negative quantity; instead of the lattice expanding upon the absorption of hydrogen the lattice contracts. The only way to understand this is by the hydrogen atom occupying a vacancy where the H-Pd distance is large enough to be in the attractive portion of the H-Pd interaction curve. Kirchheim deduced that of all structural defects vacancies in Pd provide the strongest attractive interaction with hydrogen, although a quantitative evaluation was not attained. At concentrations above 40 ppm hydrogen expands the palladium lattice (44), as already discussed, because the expansion of the normal interstitial sites overcomes the negative effect of hydrogens in substitutional vacancies. Evidence exists that vacancies interact attractively with hydrogen dissolved in copper (45) and in gold (46).

One-dimensional, or linear defects are the dislocations produced in metals by plastic deformation and many other processes. The largest body of information on hydrogen-dislocation interaction in metals that exists is for iron and its alloys. Hydrogen dissolved in b.c.c. iron is strongly held at the cores of edge and of mixed-character dislocations, and less strongly at the cores of screw dislocations (see Table 2). Additionally, hydrogen is attracted elastically to the dilatant side of edge dislocations, the interaction energy varying inversely with distance. Because other larger interstitial solutes interact more strongly with dislocation cores, hydrogen in iron does not interact with dislocations upon which nitrogen is adsorbed (49).

Kirchheim (50) has evaluated the interaction energy of hydrogen dislocations in Pd. At the core of an edge dislocation the large interaction energy (see Table 2) includes a H-H attractive interaction energy of 18.5 kJ/mol H. At larger distances from the core, the interaction energy does not have a contribution from the H-H interaction, and the remainder decreases as the reciprocal of the distance. The additional population of hydrogens due to the attractive interaction with dislocations makes a significant contribution in Pd only at very small hydrogen concentrations.

Only sparse information is available concerning interaction of hydrogen with dislocations in other metals. Thomas (51) evaluated this interaction in nickel as 9.6 to 19.2 kJ/mol. Although a quantitative evaluation was not made, Ohma et al. (54) demonstrated attractive interaction between tritium and dislocations in f.c.c. stainless steel by autoradiography. Despite the absence of data for most metals, one can be sure that in any metal that exhibits a positive partial molal volume of hydrogen there is an attractive interaction between dissolved hydrogen and dislocations, leading to highly concentrated distribution of hydrogen along the dislocation line and to smaller excess concentrations in the tensile stress region about the dislocation.

Two-dimensional structural defects in a metal lattice include stacking faults, grain boundaries, interphase boundaries and the internal surfaces of microvoids and microcracks. That hydrogen dissolved f.c.c. iron interacts attractively with stacking faults was deduced (55) from the reduction of the energy needed to create a stacking fault in hydrogen-containing iron. Grain boundaries in iron (47), in Pd (52), in nickel and cobalt (53) have been shown to adsorb excess populations of hydrogen. Mutschelle and Kirchheim (52) have shown that there is a Gaussian distribution of interaction energies between dissolved hydrogen and grain boundaries in Pd, reflecting the variety of binding sites in grain boundaries. The mean interaction energy is 5.3 kJ/mol H, with the width of the Gaussian distribution being 15 kJ/mol so that at some grain boundary sites there are repulsive interactions. The heterogeneity of binding sites on grain boundaries for tritium was qualitatively demonstrated by Laurent et al. (56) for b.c.c. iron. It seems safe to assert that grain boundaries in any metal will exhibit attractive interactions for dissolved hydrogen.

Interfaces between second-phase particles and the crystalline iron in which they reside have been shown (see Table 2) to adsorb excess populations of hydrogen. Unfortunately, measurements in other metals seem not to be available. Dissolved hydrogen will also adsorb upon internal free surfaces in metals, meaning the surfaces bounding microvoids and microcracks. These defects in metals can develop in the processing and fabrication of the metals as well as during the charging of hydrogen into the metal (see below). These internal surfaces would adsorb hydrogen to the same extent as would external surfaces of the same metallic composition in contact with the molecular hydrogen gas producing the concentration of lattice-dissolved hydrogen. In addition, the volume of the internal cavity (a 3-dimensional defect) would at equilibrium acquire a molecular gaseous hydrogen concentration consistent with the input fugacity of the external hydrogen environment.

The interactions between dissolved hydrogen in a solid metal and structural imperfections in that metal can in general be divided into two categories, chemical and elastic. The latter refers to positions sufficiently far from the imperfection so that the atomic displacements from the positions in the perfect lattice are small, and linear elasticity may be applied to a sufficient degree of approximation. The former category refers to positions where the atomic displacements are large, e.g., at dislocation cores and internal interfaces. Calculations of the excess hydrogen concentrations in the elastic region about a structural imperfection are based upon the thermodynamic relation

between the chemical potential, μ_s, of an interstitial solute such as hydrogen at a position in a solid and the stress state at that position (57). The local stress may arise as a result of externally applied mechanical forces or because of structural imperfections. In either case, the chemical potential, of an interstitial solute in the stressed body is related to the chemical potential, $\mu_s(o)$, of the solute at the same concenration in the relaxed (zero stress) body as

$$\mu_s - \mu_s(o) = \sum_i \sum_j \int_o^{\sigma_i} [V_m s_{ij} + (1-x_s)V_m \partial s_{ij} / \partial x_s]\sigma_i d\sigma_j - V_m(1-x_s)\sum_i \sigma_i \partial \varepsilon_i / \partial x_s \quad (8)$$

in which V_m is the molal volume of the solid solution of solute mole fraction x_s having the isothermal compliances s_{ij} ($=\partial\varepsilon_i/\partial\sigma_j$). The σ_i ($\sigma_i > 0$ for tensile character)are the elements of the symmetric part of the stress tensor, and the ε_i are the corresponding elements of strain.

The first term of eq. 8 leads to terms of the form $\sigma^2 \overline{V}$ /2E where E is the Young modulus; these terms are unimportant except where the stress is a significant fraction of E. Dropping the first term and using x, y and z as the Cartesian coordinates, eq. (1) may be written as (57)

$$\mu_s - \mu_s(o) = -V_m(1-x_s)\{[\sigma_{xx}\frac{\partial\varepsilon_{xx}}{\partial x_s} + \sigma_{yy}\frac{\partial\varepsilon_{yy}}{\partial x_s} + \sigma_{zz}\frac{\partial\varepsilon_{zz}}{\partial x_s}]$$

$$+ [2\sigma_{xy}\frac{\partial\varepsilon_{xy}}{\partial x_s} + 2\,\sigma_{xz}\frac{\partial\varepsilon_{xz}}{\partial x_s}\; 2\sigma_{yz}\frac{\partial\varepsilon_{vz}}{\partial x_s}]\} \quad (9)$$

The diagonal ε terms represent the fractional increase in length of elements initially parallel to the coordinate axes. The off-diagonal elements represent half the decrease of the angle between the two elements initially along the axes indicated by the subscripts. If an interstitial solute dilates the lattice isotropically, e.g., hydrogen in palladium, the off-diagonal terms of eq. (9) may be omitted, and if in addition σ_{ii}/E is small, eq. (9) reduces to

$$\mu_s - \mu_s(o) = -\frac{\overline{V}_s}{3}(\sigma_{xx} + \sigma_{yy} + \sigma_{zz}) \equiv -\overline{V}_s\sigma_h \quad (10)$$

in which $\overline{V}_s$ is the partial molal volume of the interstitial solute. The thermodynamic theory was experimentally verified by Wriedt and Oriani (17) for the case of hydrogen in silver-palladium alloy under uniaxial stress ($\sigma_{xx} = \sigma_{zz} = 0$), for which $\overline{V}_H$ was an already known quantity.

It is emphasized that the above equations relate the chemical potential of the interstitial solute in the stressed body to that in the relaxed body at the same concentration. The equations can be converted to show the variation of concentration with stress for the same chemical potential of interstitial solute in the stressed as in the unstressed body. For example, eq. (10) yields, for uniaxial stress

$$\left(\frac{\partial \ln c_s}{\partial \sigma_{xx}}\right)_{\mu_s} = (\bar{V}_s / 3RT) / (\partial \ln a_s / \partial \ln c_s)_{\sigma_{xx}} \qquad (11)$$

where a_S and c_S are the activity and concentration of solute s, respectively. Thus in an inhomogeneously stressed body, such as the neighborhood of a dislocation, the equilibrium distribution (i.e., iso-activity) of hydrogen is non-uniform, being larger at positions of greater tensile stress. Similarly a spherical particle which expands the matrix produces stresses σ_1 and σ_2 which are decreasing functions of distance, r, from the center of the particle. In the matrix the stresses σ_1, σ_2 are orthogonal to each other and to σ_r which lies along the polar coordinate with origin at the particle center. Because $-\sigma_1 = -\sigma_2 = 1/2\sigma_r$, the hydrostatic component of stress (i.e., 1/3 the trace of the stress tensor) is zero, so that only the first term of eq. (8) persists. At the surface of the spherical particle, σ_r exerts a hydrostatic negative stress (i.e., a pressure) thereby raising the chemical potential of the solid solution of the particle. Suppose that the particle is a stoichiometric hydride $MH_{n\pm\delta}$, meaning that the compound MH_n tolerates only very small values of δ, the deviation from stoichiometry. In this case, the variation of concentration with distance, r, is given by (57).

$$\frac{c_H^\alpha(r)}{c_H^\alpha(\infty)} = \exp\left[-\frac{3\bar{V}_H^\alpha}{8G_\alpha RT}\left(\frac{12G_\alpha a^3(\Delta/a)}{r^3\left(3+4K_\beta G_\alpha\right)}\right)^2\right] \qquad (12)$$

In eq. (12) α refers to the matrix and β to the hydride, G is the shear modulus and K the compressibility, a is the relaxed radius of the hydride particle, and Δ is the difference between the relaxed radii of the hydride and of the hole in the matrix. $c_H^\alpha(\infty)$ is the hydrogen concentration far from the β particle, and is larger than c_H^α in equilibrium with unstressed β. Eq. (12) shows that the c_H^α is smaller near the particle than far from it. Very complicated expressions result (58) for the case where the particle can have a wide variation of composition.

Phase Diagrams and Phase Transitions

Metal-hydrogen systems exhibit phase diagrams of varying complexity, but the purpose of this section is not to present details of individual phase diagrams but only to describe some aspects of importance to understand behavior during charging in hydrogen or evolving hydrogen from a pre-charged metal.

Effect of Isotopic Mass. The isotopic mass affects not only the concentration of hydrogen in a metal at a given temperature and hydrogen pressure (see the section called The Dissociated State of Dissolved Hydrogen) but also the composition-temperature boundaries between solid phases. The physical reasons for the effect of isotopic mass on phase boundaries are related to differences in the zero-point energies of the dissolved hydrogen isotopes, the differences in the lattice expansions produced

by the isotopes, and the differences produced in the phonon spectrum. The reader is referred to ref. 18 for discussion of specific cases.

Effect of Lattice Stresses. The large mobility of hydrogen dissolved in a lattice, the metal atoms of which are virtually static by comparison, makes it very probable that the transition from one phase to another will initially be accomplished by the motion of only the hydrogen atoms. Consider the Pd-H system. Below the critical temperature of 292°C, this system is characterized by a miscibility gap within which two f.c.c. phases of different composition coexist. The one with the lower hydrogen content, usually called the α-phase has at 20°C $n_H / n_{Pd} = 0.008$ whereas the hydrogen-rich phase, usually termed the β-phase, has $n_H / n_{Pd} = 0.607$. The H_2 gas pressure in equilibrium with these co-existing solid phases is about 0.07 atm (59). The α and β phases have the same lattice symmetry (strictly speaking they represent portions of one phase field) but very different specific volumes; the change of volume for the transition $\alpha \rightarrow \beta$ is in fact 1.57 cm^3/mol H (8). Hence the transition involves a clustering together of hydrogen atoms such that 125 Pd atoms which in the α-configuration have only one H atom among them, in the β-configuration the 125 Pd atom cluster has nearly 76 H atoms for which the lattice parameter is 0.4025 nm instead of 0.3894 nm.

Because this cluster of Pd atoms has expanded within the α-phase, mechanical stresses must be generated analogously to the misfitting ball-in-hole model discussed in a previous section. The only way to mitigate the stresses is by removing Pd atoms of the surrounding α-phase to the external surface of the specimen. Hence, two extreme (or idealized) cases exist, one in which the stresses are not at all relieved and the other in which all stresses are relieved. This gives rise to two kinds of equilibrium, and hence to two kinds of phase diagrams the coherent and the incoherent equilibrium diagrams. It is emphasized that these are idealizations and that in practice a phase distribution of mixed character is achieved, the degree of stress relief being dependent on details of the experimental procedure.

In the idealized coherent equilibrium between two phases of a metal-hydrogen system one phase has grown within the parent phase without any diffusive motion of the metal atoms and without any plastic deformation. Hence, the lattice lines are continuous, although not straight, between one phase and the other, and the interface between the two is characterized by a change of composition and an inflection point in the lattice parameter-distance variation. The resulting coherency stresses change the chemical potential of the dissolved hydrogen in both phases along the principles described in a previous section, so that the compositions of the coexisting phases in equilibrium with a given hydrogen gas fugacity have values different from those that would exist in the absence of stresses at the same hydrogen gas fugacity. Furthermore, for a single crystal with free surfaces the compositions of coherent coexisting α and β phases would be functions of the shape of the crystal (60). This results from the coherency stresses being functions of the image forces at the free surfaces. For a long thin wire the effect of coherency stresses is negligible so that the compositions of coexisting coherent phases would be the same as for a fully incoherent equilibrium.

The coherent equilibrium is in general a metastable condition of higher free energy because of the elastic energy, than that of the corresponding incoherent equilibrium. The change from coherency to incoherency necessitates the nucleation of dislocations which can move the matrix atoms, by slip, away from the neighborhood of the coherent second-phase particle to free surfaces or to grain boundaries. The nucleation cannot occur until enough coherency elastic energy has accumulated by the growth of the coherent particles to "pay" for the self-energy of the dislocations. In general, coherency is lost by the formation of dislocations at the interface between the α and β phases and by the generation of dislocations which ideally should carry metal atoms to the free surface or to grain boundaries. However, this transport is never complete, so that the system usually ends up with large dislocation densities distributed throughout the metal grains. Although the excess free energy in the coherent equilibrium is considerably reduced by the transition to incoherence, it is not totally removed since the dislocations represent a free energy excess over the dislocation-free state. The coherence-incoherence transformation is the chief reason for the well-known hysteresis observed when trying to establish phase boundaries in metal-hydrogen systems. Coherency stresses and their reduction by dislocation generation occurs both in hydrogen charging into, and discharging from, a metal whenever more than one phase is produced by the ingress or egress of hydrogen (18, 61). The generated dislocations modify the mechanical properties, as is discussed in a subsequent section, and can affect microcracking of the metal.

Kinetic Aspects of Dissolved Hydrogen

Diffusion in the Volume of the "Perfect" Lattice

It is well known that hydrogen in metals diffuses more rapidly than any other solute. It may be less widely recognized that the mechanism of the rapid diffusion is not fully understood. Because hydrogen atoms have small masses quantum effects can be expected to play a role, and the fact that the activation energy for the diffusion of hydrogen in Nb, Ta, and V is a function of isotopic mass strengthens this expectation.

Kehr (62) points out that four different diffusion mechanisms should be considered for hydrogen in metals. At the lowest temperatures, hydrogen may be delocalized as a band state and its propagation in the band state would be limited by scattering by phonons and by lattice defects. At higher temperatures hydrogen is localized at specific interstitial positions and thermal energy is required to change location. One possibility is tunneling from one to another interstitial site, thermal energy being needed to bring the energy levels of both sites to the same value. The second possibility for hopping involves an activation energy to go over the energy barrier between sites. This is the classical mechanism of diffusion, and should be dominant at higher temperatures. At the highest temperatures the hydrogen would populate states above the energy barriers and its diffusion would resemble the diffusion in a dense gas or liquid. Many collisions would occur with the thermal fluctuations of the host lattice. The temperature regimes in which one or another mechanism operates are not sharply defined. This paper does

not discuss the degree to which experimental measurements support one or another mechanism. Readers interested in this aspect are directed to refs. (62) and (2).

Table 3 collects diffusivity data for the isotopes of hydrogen at low concentrations in various metals in terms of the pre-exponential term, D_o, and the activation energy, E_a, of the Arrhenius equation $D = D_o \exp(-E_a/RT)$. We note that the ratio of diffusivity of H and D in Pd does not follow the classical prediction that $D_H/D_D = (m_D/m_H)^{1/2}$, and furthermore the E_a depends on isotopic mass. This deviation is not fully understood, but it is affected by the difference in the anharmonic character of vibration of the hydrogen isotopes.

The diffusivity of H in Pd, in PdAg alloys, and in Nb and Ta is a weak function of hydrogen concentration, generally decreasing with increasing hydrogen. Most of the reason for this dependence is the non-ideality of the metal-hydrogen solid solution. The diffusivity as measured by the relaxation of a concentration gradient, is defined as

$$D = kTB(d \ln a/d \ln x) \qquad (13)$$

where x is the mole fraction of the mobile solute and a is its thermodynamic activity. B is the mobility of the solute. Because the relation between activity and concentration varies with concentration, D will vary. If a high hydrogen concentration is achieved by equilibrium with high pressure gaseous hydrogen one may ask if the compression of the lattice by the imposed pressure affects the mobility. Baranowski (68) asserts that this affect is small. The mobility can also be concentration dependent because with increasing hydrogen concentration the number of vacant interstitial positions into which the hydrogen can jump diminishes, and also the metal atom-hydrogen interaction changes as the lattice expands with increasing hydrogen concentration. A particularly interesting and large effect of hydrogen concentration on the diffusivity is observed in the vicinity of the critical concentration and temperature. In that region the diffusivity of hydrogen can decrease by several orders of magnitude because d ln a/d ln x approaches zero. The mobility is not anomalous in that region.

The Arrhenius relation is not obeyed over the investigated temperature range by H in Nb (63) but it is obeyed by D in Nb. Disobedience is found also for H and D in Ta. These deviations from the Arrhenius relation are thought to be related to changes in the mechanism of diffusion.

Two- and One-Dimensional Diffusion

Despite the importance of the diffusion of hydrogen, both in molecular and atomic forms, upon external surfaces of metals to the understanding of the absorption of hydrogen from the gas phase into the lattice, very little data exist on this topic. Gomer et al. (69) applied field emission microscopy to hydrogen on a tungsten surface, and found that hydrogen exhibits a mobility dependent on the degree of surface coverage. At coverages larger than one-half monolayer the activation energy for migration is 25

kJ/mol H, but as coverage decreases the activation energy rises to 40, and at very low coverages to 67 kJ/mol H. The reason for this variation is that at low coverages only sites characterized by large adsorption energy are occupied; the adsorbed hydrogen is tightly bound so that its mobility is restricted. Larger coverages put hydrogen on surface sites with smaller binding energies so that the mobility is greater. Nickel was also investigated by the same group (70) who found 30 kJ/mol H for the E_a of surface diffusion of hydrogen independent of coverage. This was interpreted as showing that there are very few tight-binding sites on the surface of the nickel. This is reasonable because the field-emitter tip of this f.c.c. metal consists of terraces and steps of only close-packed layers. From the data one can calculate that at 37°C, $D_H \approx 4 \times 10^{-8}$ $cm^2 s^{-1}$, which may be compared with $D_H = 4.5 \times 10^{-9}$ cm^2 s^{-1} for the diffusivity of hydrogen in the volume of Ni at the same temperature (71).

The same picture as for tungsten emerges in the investigation by Arantes et al. (72) of the diffusion of hydrogen along grain boundaries in palladium. By using nanocrystalline Pd they showed that at very low hydrogen concentrations. D_H in grain boundaries is about 1/10 of D_H in the volume, but the grain boundary diffusivity becomes larger than the volume diffusivity at larger coverages because grain boundary sites of smaller binding energy become occupied. At still higher coverages the D_H along grain boundaries decreases because of the attractive interactions between adjacent hydrogens. Overall, D_H along grain boundaries in Pd is 10 to 100 times larger than in the volume. A greater D_H along grain boundaries has been observed also in nickel (73).

Seebauer et al. (74) measured the diffusion of deuterium atoms on surfaces of platinum and rhodium. They found that on Pt the activation energy and the pre-exponential term decrease with increasing coverage, producing an increasing diffusivity with increasing coverage. On Rh, however, the activation energy increases somewhat with increasing coverage, while the pre-exponential term remains essentially constant. It may be that attractive D-D interactions produce the predominant effect in the case of rhodium.

The diffusivity of hydrogen along dislocation lines in palladium (the so-called "pipe diffusion") has been evaluated by Kirchheim (50) as about ten times the D_H in the volume.

Diffusion with Trapping

The concept of trapping (i.e., the short-or long-time detainment of a solute in diffusive motion) originated in the attempt to understand the tremendous decrease of the diffusivity of hydrogen in steels as a result of plastic deformation (75). Any structural imperfection (Table 2) or impurity atom (Table 4) with which dissolved hydrogen interacts attractively will cause the hydrogen atom to spend more time in its vicinity than at a normal lattice site, chiefly because the activation energy for escape from a tight-binding site will be increased approximately by the binding energy. Specific kinetic models for this effect have been constructed (81), as well as models which assume equilibrium between the trapped and untrapped populations (82). The reduction of diffusion of hydrogen by trapping has been measured in iron and steels by

dislocations (see refs. 82, 47) and by Ti and TiC interface (80); in palladium by dislocations (83), in vanadium by dissolved oxygen and titanium (78), and in niobium by dissolved oxygen and vanadium (77). Although direct experiments with other metals do not seem to exist it is safe to expect the trapping-reduced diffusivity to be a general phenomenon, which increases in importance as the normal lattice-dissolved concentration of hydrogen decreases.

Dislocation Drag

That moving dislocations can transport hydrogen faster than can motion by diffusive transport was first suggested by Bastien and Azou (84). The permeability of hydrogen during the plastic deformation of nickel was found (85) to increase the apparent diffusivity by five orders of magnitude; this was interpreted as transport of trapped hydrogen by moving dislocations. Louthan et al. (85, 85) observed that a stainless steel absorbed more tritium from the gas phase when the steel was deformed, and autoradiography showed that the tritium was enriched at slip lines. It was proven that the greater absorption was due to enhanced transport and not easier surface entry by investigating different surface finishes.

Although investigated in just a few metals, the mechanism of the drag of hydrogen by dislocations moving in response to stress can be confidently expected in other metals. It will be important in metals in which the product of lattice-dissolved hydrogen concentration and diffusivity is small.

Diffusion Driven by Gradients Other Than of Composition

Stress Gradients. Isothermal diffusion is a flux produced by the biasing of the random jumping of an atom (or a molecule) by a thermodynamic driving force, grad μ, where μ is the chemical potential of the mobile solute. The chemical potential is influenced by all the force fields that can affect the free energy of the solute. For the uncharged (neutral) dissolved hydrogen in a metal, under the conditions for which eq. (10) is valid, the diffusion flux can be written

$$J = -Bc\,grad\mu \tag{14}$$

$$= -B\left[RT\left(1+\frac{d\ln\gamma}{d\ln c}\right)\right]gradc + Bc\bar{V}grad\sigma_h$$

$$= -D\left(gradc - \frac{c\bar{V}}{RT}grad\sigma_h\right) \tag{15}$$

in which we have used eq. (13) as well as the Einstein relation D=BRT.

Thus, at zero grad c, stress-induced hydrogen diffusive flux will occur whether the inhomogeneous stress is caused by externally applied forces, by stress fields caused by second-phase particles, dislocations, or by the inhomogeneous distribution of dissolved hydrogen. In the latter case both grad c and grad σ_h will be operative. It should be emphasized that eq. (15) represents the simplest possible case; in the general case, gradients of the off-diagonal terms of the stress tensor must also be included (see eq. 9). The effect of stress gradients is not trivial. It can be shown (48) that the Δc that would just cancel a $\Delta\sigma_h$ is given by $\Delta\sigma_h/\Delta c = RT/c\overline{V}$ for the case where $d\ln\gamma/d\ln c = 0$. Letting $\Delta c = c - 0 = c$, $\Delta\sigma_h = RT/\overline{V} = 1.49 \times 10^{10}$ dyne/cm^2 at room temperature and for $\overline{V}$ = 1.68 cm^3/mol as in palladium. This is a smaller stress than that existing two Burgers vectors away from the core of an edge dislocation on its tensile side.

Electrical Potential Gradient. If one produces an electrical field gradient in a Pd(H) solid solution a flux of electrons results. Another consequence is that a flux of the dissolved hydrogen also occurs. This is an example of cross effects in diffusion as treated in the thermodynamics of irreversible processes (87). The production of a flux of metal-dissolved solute caused by the flux of charge carriers is called electromigration. It cannot be understood as a response to a thermodynamic driving force as it is in fact a kinetic phenomenon. In the absence of concentration and stress gradients, the flux of hydrogen in an electrical potential gradient, grad ϕ, is

$$J = cBF \equiv cB\, Z^* \text{ grad } \phi \qquad (16)$$

where Z^* is called the effective charge of the hydrogen in units of the electronic charge. Z^* is negative if the solute moves in the same direction as the electrons under the applied grad ϕ. Although full understanding of electromigration is not yet available (88), it can be said that Z^* is the sum of two effects: a "direct field effect" whereby the screened ion experiences a force from the grad ϕ, and a "wind effect" meaning that charge carriers (both electrons and electron holes) moving in response to the field transfer momentum to the solute atom. The view of this writer (89) is that the momentum transfer and the direct-field effect at the saddle point of the activated state are the relevant quantities to be considered. Irrespective of the details of the mechanisms embodied in the effective charge it is clear that the magnitude and sign of Z^* are not simply related to the "ionicity" of the dissolved hydrogen in its ground state. Table 5 collects some measured values of Z^* of hydrogen; where a range of values is given it is because Z^* was found to be temperature dependent. Attention is directed to the several negative values of Z^* and to the temperature dependence in some cases, neither of which is understandable in the absence of a momentum-transfer contribution. The force F_ϕ upon dissolved hydrogen arising from an electrical potential gradient of 1 volt cm^{-1} is 6×10^{-13} dyne/atom, using $Z^* = 0.5$ for H in Pd. This may be compared with the force arising from a concentration gradient: $F_c = 4.1 \times 10^{-14}$ dyne/atom, calculated for (1/c) grade = 1 cm^{-1} at 295 K, so that the electromigration force is not insignificant.

Temperature Gradient. Another example of cross effects is the migration of solutes in metals caused by a temperature gradient, called thermomigration, or thermotransport. The force upon a solute due to a grad T is $F_T = (Q^*/T)$ grad T, where Q^* is called the

heat of transport. For Q^*=.065 eV for H in Pd, T = 700°K and grad T = 100°K/cm, $F_T=10^{-14}$ dyne/atom. The heat of transport is more complex than Z^* because the applied grad T produces fluxes of charge carriers and of phonons all of which interact with the solute in its activated state. In a metal, momentum transfer from collision with the charge carriers is probably the more important (90).

Phenomena Accompanying Input and Egress of Hydrogen

With Molecular Hydrogen Gas

The transition between the gaseous molecular state and the lattice-dissolved screened-ion state must involve the sequence: impingement of H_2 molecules of the gas upon the surface, adsorption of the H_2 molecule, dissociation into adsorbed H atoms, and transition between the adsorbed and the absorbed (dissolved) state. The details vary from metal to metal, and also from one type of crystallographic surface plane to another type for any one metal. Therefore, it is possible in this review only to indicate some generalities and to go into some detail for only one metal.

The rate of impingement of gaseous molecules is well described by the kinetic theory of gases. The fraction of the impinging molecules that stick (the sticking coefficient) is relatively small because the adsorption energy of the molecule is small. The molecule must diffuse along the surface to a position where the dissociative adsorption can proceed. The adsorption of the molecule and its dissociation are strongly impeded by pre-adsorbed species such as oxygen, nitrogen and atomically adsorbed hydrogen. The dissociation of the H_2 molecule upon a surface oxide is very difficult, so that virtually only metal atoms at the surface are effective. Finally, the adsorbed atoms must diffuse from the dissociation sites to locations on the surface providing low kinetic barriers for the passage from the surface to the interior of the lattice. Each of these steps is a strong function of the atomic topography of the metal surface, i.e., atomic steps, kinks on the steps, and surface vacancies. Further movement into the lattice proceeds by diffusion, the boundary condition for which is set by the concentration, c_o of dissolved hydrogen in the first lattice plane below the surface.

Some details can be given for hydrogen on palladium. Aldag and Schmidt (91) found very small sticking coefficients below 100 K, but at higher temperatures the coefficient rises to about 0.1. These investigators found four states for chemisorbed molecules on polycrystalline Pd with adsorption energies ranging from 54 to 146 kJ/mol H. Conrad et al. (92) found that the chemisorption of H_2 molecules increases the work function of Pd, so that the adsorbed species receives a net electron transfer from the metal. In this state the H atoms on Pt (111) planes are situated above triangles of Pt atoms forming an octahedral plane of their own with an interatomic separation of 0.0962 nm (93), compared with 0.0742 in the undistorted H_2 molecule. It is considered that dissociative chemisorption on Pd(111) proceeds in the same configuration. The absorption into the lattice does not proceed from the octahedral sites, however. The dissociated H atoms must diffuse (94) to the weak binding sites on the surface that correspond to tetrahedral sites in the bulk Pd lattice and to Aldag and Schmidt's weak binding sites. These sites

also correspond to the weak chemisorption investigated by Lynch and Flanagan (11). From these surface sites the adsorbed atoms make their entry into the lattice (94), and since these are also the sites of the initial adsorption of H_2 molecules, occupation of these sites by H_2 molecules interferes with the surface-to-volume transition of the adsorbed atoms. The rate-determining step for the whole process was found (94) to be the dissociation of the adsorbed H_2 molecule. Similarly, the rate of egress from the lattice dissolved state into the gaseous phase is kinetically limited by the rate of recombination. If adsorbed oxygen, or adsorbed C_2H_5, or other groups that can react with adsorbed hydrogen are present on the Pd surface, H-H recombination is not needed (94). It should be pointed out that in the absence of such reactive groups (which can have only a transient effect) whatever impedes the input of hydrogen should also impede the egress. This is an inference from the principle of microscopic reversibility, that the sequence of steps in the forward direction must be reversed for the backward direction. It should also be noted that whereas adsorbed species can affect the rates of ingress and egress of hydrogen, they do not affect the equilibrium concentration produced in the lattice at a given temperature and gas fugacity.

With Sources of Hydrogen Atoms

The dissociation of the H_2 molecule on the metal surface can be circumvented by depositing directly hydrogen atoms. This may be done by exposing the surface to a partially dissociated gas produced by a variety of techniques. The equilibrium ratio of H atoms to H_2 molecules in hydrogen gas at room temperature is 10^{-30}, but the concentration can be increased by many orders of magnitude in the immediate neighborhood of, for example, a hot tungsten wire. However, recombination occurs in the gas phase, on the walls of the containment chamber, and most importantly on the surface of the metal to be charged with hydrogen. For this reason, and also because there is not thermal equilibrium between the atoms and the molecules in the gas it is not possible to calculate a thermodynamic fugacity of the partially dissociated gas whereby to evaluate the driving force (i.e., the free energy change) for the process H(gas) $\rightarrow$ H(metal). In practice, it is possible to achieve much larger concentrations of hydrogen in metals by the use of partially dissociated hydrogen gas than with molecular gas at ordinary pressures. For example, nickel hydride (NiH) can be produced (95) by impinging H atoms on nickel at 25°C. Since a molecular gas pressure of 6 kbar is needed (68) at 25°C to produce NiH one may infer that the input fugacity of the dissociated gas in the experiment of ref. 80 was that corresponding to 6 kbar pressure. (The concept of input fugacity is discussed below). The concentration that may be reached in a metal by exposing it to a partially dissociated gas is very sensitive to surface contaminants and experimental conditions; this has not been studied systematically.

Electrolysis also deposits hydrogen atoms on the metal surface. In the case of aqueous electrolytes the deposition reaction can occur by the reduction of water or of hydronium ion. From fused salt electrolytes the hydrogen atom results from the oxidation (96) of the negative hydride ion. In either case the population of hydrogen atoms at the metal-

electrolyte interface is controlled by the kinetics of the recombination of the hydrogen atoms in competition with the kinetics of the transition between the surface state and the absorbed state. the recombination apparently occurs preferentially on specific surface sites having a distinctive atomic topography. For example, Stackelberg and Bischoff (97) found that on palladium bubbles of gaseous hydrogen form almost exclusively at grain boundaries on the surface, and Storms et al. (98) found that 7.6 wt % carbon in Pd significantly reduces the uptake of deuterium, although the mechanism of this effect was not elucidated. The rate of entry of hydrogen into iron can be increased over the rate of recombination to form gaseous hydrogen by various chemicals added to the electrolyte which apparently block the sites preferred for the recombination reaction. Such chemicals are certain compounds of elements of the V-A and VI-A groups of the periodic table. The precise way in which these compounds promote the entry of hydrogen into iron is still under investigation, although a well supported idea in that formation of the hydride is an essential step (99,100). Promoters of hydrogen entry into palladium have not been clearly identified. For example, Riley et al. (101) obtained contradictory results using various electrolytic solutions.

Promoters of hydrogen entry affect not only the rate of entry but can, in some circumstances discussed below, also control the steady-state hydrogen content attained within the metal. The rate of entry diminishes with increasing hydrogen content already in the metal. An extreme example of this is furnished by hydrogen charging from the gas phase (102) into titanium. If the gas fugacity is high enough to produce a hydride phase near the input surface, penetration of dissolved hydrogen deeper into the metal is seriously impeded by the low diffusivity of hydrogen in the hydride. Another impediment to the penetration of hydrogen beyond the immediate vicinity of the input surface is the generation of dislocations and other defects (see below) that can trap the incoming hydrogen.

Input Fugacity of Hydrogen

It has already been stated that with molecular gaseous hydrogen the thermodynamic driving force for the transition between the gaseous state and the lattice-dissolved state in a metal, and also the concentration of dissolved hydrogen at equilibrium, are fixed at any one temperature by specifying the fugacity of the gas (this neglects hysteretic phenomena) irrespective of surface conditions. Although this cannot be done in the cases of electrolytic charging or of partially dissociated or ionized hydrogen gas, it is sometimes useful to speak of the input fugacity, or effective fugacity, of the incoming hydrogen. Both methods of charging produce a population of adsorbed hydrogen atoms on the surface of the metal that is kinetically controlled as discussed previously. At steady state, such that the surface population everywhere on the metal surface and the concentration of hydrogen within the metal are uniform and independent of time, and furthermore the defect structure of the metal is independent of time, then one can say that there is thermodynamic equilibrium among all of the states of hydrogen within and upon the surface of the metal, but not between these states and the source of the hydrogen. In these circumstances, the lattice-dissolved hydrogen concentration, c^L everywhere in the metal can be related to the fugacity, f, of the molecular gas that at the

same temperature would produce at equilibrium the same value of c^L. That value of f is termed the input fugacity, f_i, produced by the charging system at its operating parameters, which include not only (for the electrolytic case as an example) the cathodic current density but also the composition of the electrolyte, its hydrodynamic state, the nature of the metal, and the chemical and structural state of the surface of the metal.

The identification of f_i from the c^L involves the thermodynamic relationship $c^L\left(f_{H_2(g)}\right)$ which at very large fugacities may not obey Sieverts' law because of H-H interactions in the dissolved state. Of course, f_{H_2} and the pressure, p_{H_2}, of the gas are thermodynamically related as shown by Table 6 (103). It should be clear that defining an f_i from the c^L by assuming that the f_i (c^L) relation is the same as the $f_{H_2}(c^L)$ relationship does not imply that the metal with the steady-state c^L under cathodic charging is itself under the hydrostatic pressure consistent with the thermodynamic function $f_{H_2}(p_{H_2})$ for the gas. Under steady-state electrolytic charging or dissociated gas charging, the pressure upon the metal is the environing pressure. Furthermore, the H atoms within the metal experience only the mechanical reaction from the lattice associated with the expansion of the interstitial site that manifests itself as the partial molal volume. There is no external pressure, p_{H_2} coordinated with f_i, and in particular there is no force tending to push H atoms to smaller separations or to cause double occupancy of any one interstitial site. Because the metal under gaseous molecular hydrogen of fugacity f_{H_2} producing c_L is under a compression produced by the p_{H_2} that corresponds to f_{H_2} whereas the metal with steady-state dissolved concentration c^L produced by cathodic charging does not experience an external pressure p_{H_2}, the assumption that the functional relationship f_i (c^L) is identical with f_{H_2} (c^L) cannot be completely correct. However, at $f_{H_2} = 10^7$ atm, $p_{H_2} = 12 \times 10^3$ atm, and using a typical compressibility for metals of -5×10^{-7} atm^{-1}, the fractional volume change $\approx 6 \times 10^{-3}$, so that the volume compression caused by the molecular gas is small.

A technique that has been applied (49,104,105) to evaluate f_i in cathodic charging is to measure the steady-state permeation of hydrogen from which c_0^L, the sub-surface input concentration of hydrogen can be calculated if the diffusivity of hydrogen in the bulk of the metal is known. Again, the functional relationship $c^L(f_{H_2})$ is assumed to relate c_0^L to f_i. Note that this technique does not depend on equilibrium between the adsorbed population of hydrogen and the sub-surface concentration. Another way of putting this is that the technique for evaluating f_i does not depend on whether or not the permeation is under diffusion control. However, the technique depends on achieving steady state in all respects.

Development and Relief of Stresses

Coherency Stresses. That dislocations are produced in metals by diffusion of solutes, and by inference that stresses are produced by diffusion, has been realized for a long time. Schwuttke and Queisser (106) observed dislocations after the diffusion of Ga, B and P in silicon. Electron microscopy was used to study dislocations produced in silicon by the diffusion of B (107) and of P (108). Some calculations of diffusion-induced

stresses were made by Prussian (109) but Li (110) has made the most detailed calculations.

Consider a thin slab of thickness 2a in which an interstitial solute of partial molal volume, $\bar{V}$, is diffusing only in the thickness direction, x, towards the center, the boundary condition being a constant sub-surface solute concentration, c_o, for $t \geq 0$ and $c = 0$ at $t = 0$ everywhere except at the sub-surfaces. For constant Young's modulus, E, and Poisson ratio, ν, and in the absence of any plastic deformation, the stresses in the orthogonal directions normal to the thickness direction are given by (110)

$$\sigma_{yy} = \sigma_{zz} = \frac{2\bar{V}c_o E}{3(1-\nu)} \sum_{n=0}^{\infty} \frac{1}{\rho_n} \left[(-1)^n \cos\left(\frac{n\pi x}{a}\right) - \frac{1}{\rho_n} \right] \exp\left(\frac{-\rho_n^2 Dt}{a^2}\right) \qquad (17)$$

in which c_o has units of moles cm^{-3}, $\rho_n \equiv (2n + 1)\pi/2$ and D is the diffusivity of the solute. This equation is plotted in Fig. _. The dashed lines represent the envelope of all the curves. It may be shown that the maximum stress developed by diffusion is

$$\sigma_{max} = -\frac{\bar{V}c_o E}{3(1-\nu)} \qquad (18)$$

Fig. 1 shows that it occurs at the input surfaces at the start of the diffusion ($\sigma > 0$ is tensile, $\sigma < 0$ is compressive).

Assume now a similar slab geometry with solute diffusing in from a constant subsurface concentration from only one surface, the other surface blocking the out-diffusion of the interstitial solute. The stress-time relationship is given by (111)

$$\sigma_{yy} = \sigma_{zz} = \frac{2\bar{V}Ec_o}{3(1-\nu)} \sum_{n=0}^{\infty} \frac{1}{\rho_n} \exp\left(\frac{-\rho_n^2 Dt}{(2a)^2}\right) \left[\sin\left(\frac{\rho_n x}{2a}\right) - \frac{1}{2\rho_n} - \frac{3}{\rho_n^2} \sin\rho_n + \frac{3}{\rho_n^3} \right] \qquad (19)$$

and again the maximum stress is given by eq. (18) and occurs at the input surface at the start of diffusion. The expansion caused by the dissolution of hydrogen places the input region in compression because of the constraint by the underlying unexpanded hydrogen-free metal, and the plate develops concavity towards the blocked surface. As diffusion proceeds the stresses decrease. For the case of steady-state diffusion with solute going in at one surface and going out the other, as is the case in a typical hydrogen permeation experiment, if $\bar{V}$ and E are constant the resulting steady-state linear c(x) profile produces zero stresses.

Another geometry that is common in cathodic charging of hydrogen is that of a cylinder, at the cylindrical surface of which the solute concentration is held at c_o and at $t = 0$, $c = 0$ everywhere else. Fig. 2 shows the shear stress as a function of position (r is measured from the central axis of the cylinder and a is the cylinder radius) and time. The largest shear stress is at the input surface, which, calculated for palladium at a c_o corresponding to $D/Pd = 0.65$ at $Dt/a^2 = 0.01$, is about 4×10^9 Pa, which is much larger

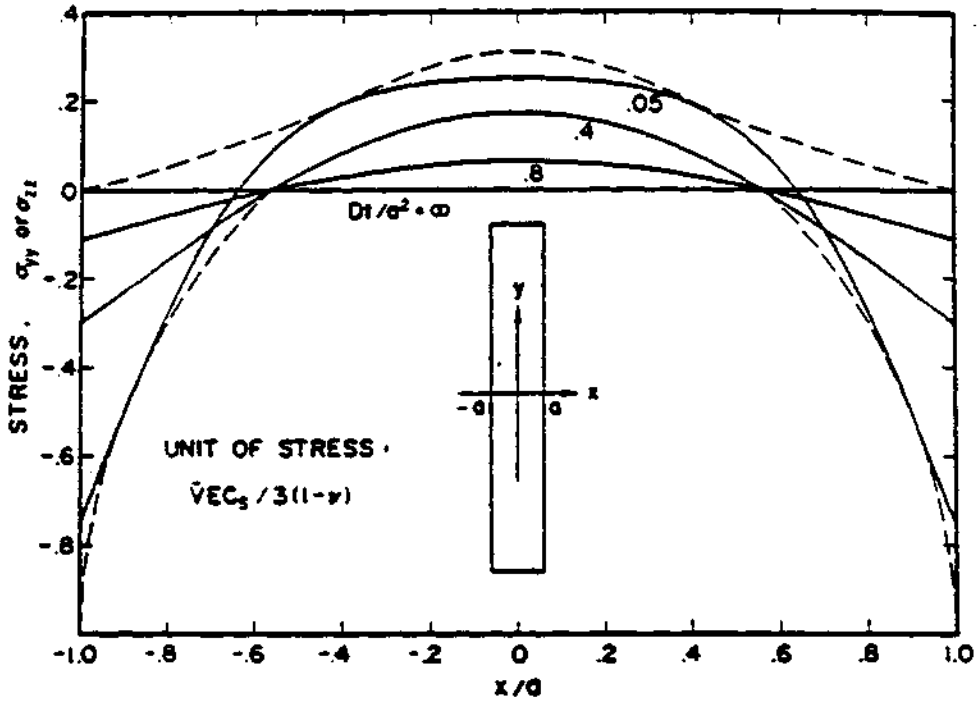

Figure 1. Stresses produced by the diffusion of hydrogen into both sides of a thin slab (Ref. 10).

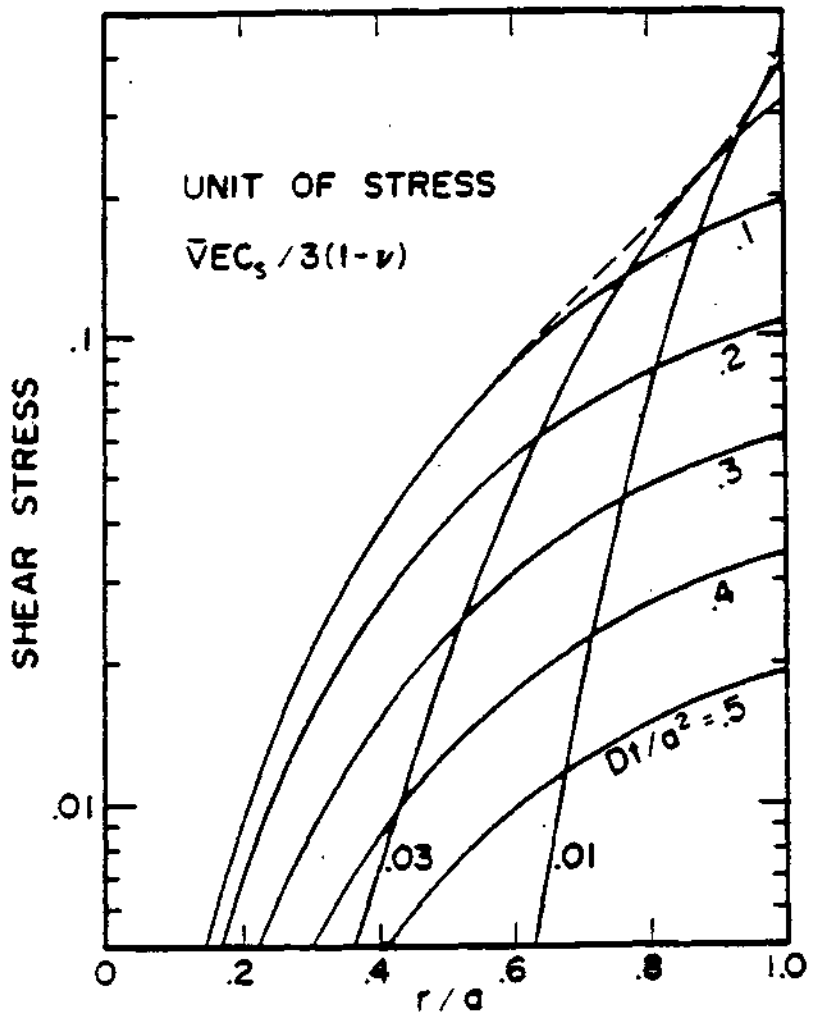

Figure 2. Shear stress produced by the diffusion of hydrogen into a thin cylindrical metal (Ref. 10).

than the yield stress of the metal. Hence, one must expect dislocations to be generated and to move in the stress gradient.

The above equations for stress are first-order calculations in the sense that diffusion is considered to be motivated only by a concentration gradient; no account is taken of the stress gradient itself affecting the driving force for diffusion. Improved calculations can be made by substituting for D in the stress equations an effective diffusivity given by

$$D = D_o\left[1+\left(\frac{\partial \ln x}{\partial \ln c}\right)+\frac{2c\bar{V}^2E}{9RT(1-\nu)}\right] \qquad (20)$$

derived by Li(110) for cases when stresses are caused only by diffusion. This equation includes the correction required for the concentration dependence of the activity coefficient, γ. Because in these geometries the gradient of the hydrostatic component of stress is proportional to the concentration gradient the stress-modified effective diffusivity is larger than the ordinary diffusivity.

Heterogeneous Generation of Dislocations. That the in-diffusion of hydrogen of hydrogen can generate stress larger than can be supported by the metal, even in the absence of phase changes, has been demonstrated experimentally (111) with a b.c.c. alloy, Ti-30 Mo which remains single phase with hydrogen contents up to about an atomic ratio of 0.6. In these experiments hydrogen was cathodically charged into only one side of a thin sheet of metal. Transmission electron microscopy showed very large density of dislocations distributed at random, in clusters and in networks (Fig. 1). The dislocation cluster in the left-hand side of Fig. 3 has a dislocation density about 1000 times that in an annealed sample, and resembles the clusters of dislocations found in nickel (112) after the diffusion of carbon. There are also pile-ups of dislocations at grain boundaries far from the input surface (Fig. 4); this is important because dislocation pile-ups can nucleate microcracks, and it shows that the diffusion-induced stresses cause the generated dislocations to glide into metal that is as yet free of hydrogen. Fig. 3 demonstrates that most of the dilocations are along slip planes in accord with similar findings in other systems after interstitial diffusion (113).

In addition to the generation and motion of dislocations that relax the stresses produced by the in-diffusion hydrogen into Ti-30 Mo alloy, other interesting phenomena were observed (111). The change of lattice parameter with diffusion time was measured for various grains of the polycrystalline alloy in the surface of the specimen that was not in contact with the electrolyte employed for the cathodic charging . It was found that the changes continued to occur over durations of hydrogen charging that were far longer than the time required for Fickian diffusion to have reached a steady state. This can be explained only by the trapping of hydrogen by the generated dislocations. Furthermore, the change of lattice parameter was different in different crystal grains (Fig. 5), and also the intensity of various Bragg peaks changed with time of charging. Indeed, to obtain maximum intensity for a given Bragg peak it was necessary to rotate the sample with respect to the x-ray detector and source. The necessary rotation was a

Figure 3. Clusters of dislocations produced in Ti-30 Mo alloy by cathodic charging of hydrogen (Ref. 111).

Figure 4. Dislocation networks and pile-ups at grain boundaries in Ti-30 Mo alloy after cathodic charging (Ref. 111).

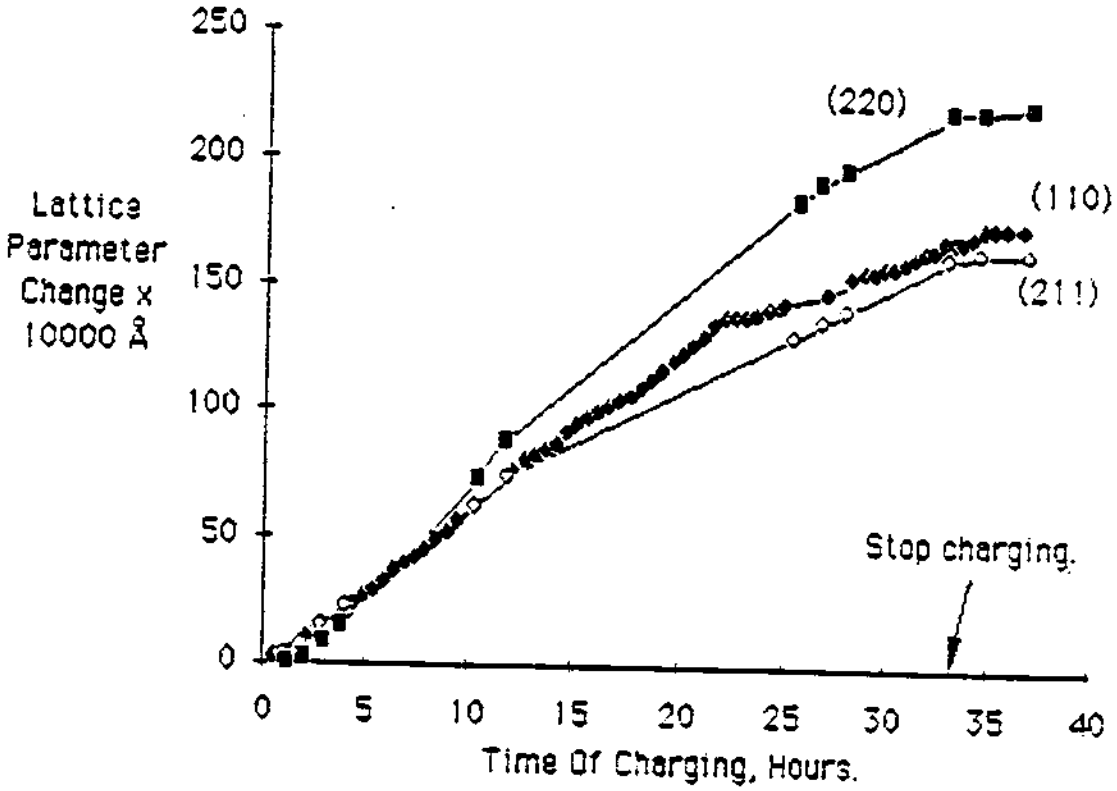

Figure 5. Change of lattice parameter with time of cathodic charging of hydrogen into one side of a Ti-30 Mo plate. The various Bragg reflections were taken from the side of the plate far from the input surface (Ref. 111).

function of time during charging and the dependence on time was different for different crystal grains (Fig. 6).

Recalling that the change of lattice parameter in any one grain reflects the change of dissolved hydrogen concentration in that grain, one concludes that at a given distance from the input surface, the lattice-dissolved hydrogen concentration was different in different grains. The rotation of the sample to obtain maximum intensity of any one Bragg peak means that the angular positions of the diffracting crystal planes were changing during charging. Other defects produced by hydrogen charging are deformation bands and microcracking at the far surface of the specimen. Deformation bands probably formed by accumulations of edge dislocations of the same sign on slip planes. Their formation in polycrystalline metals during deformation is known to be facilitated by the restraints imposed by grain boundaries. Circular protruberances were also found both on the input and the far surfaces. These were especially prominent in the tentalum and niobium specimens that were also studied (111).

These observations may be explained by the generation of dislocations, near the input surface initially, which trap the charged-in hydrogen; consequently the c_0, controlling Fickian diffusion beyond the dislocated region, is initially small. As the dislocation density increases in that region their mutual interactions grow so that the local flow stress increases, the rates of dislocation generation and of hydrogen trapping decreases. Consequently, c_0 increases so that the diffusion flux into the rest of the specimen thickness increases. This is responsible for the slow increase of hydrogen concentration, and hence of lattice parameter, at the far side of the specimen. At the same time, the shear stress at the input surface causes dislocations to glide towards the far side, carrying trapped hydrogen with them. This hydrogen is distributed to grain boundaries, to dislocation pile-ups at barriers and to grain interiors where they increase the lattice parameter, adding to the effect from diffused hydrogen. As the dislocations move away from the input side they interact with each other and with grain boundaries, annihilating each other, forming pile-ups some of these breaking through grain boundaries and others producing microcracks, and causing changes in grain boundary configuration. All these effects depend on the orientation and type of grain boundary, so that the distribution of the hydrogen, conveyed either by diffusion or by dislocation transport, between the volume of a grain and its boundary is a function of grain orientation in the specimen. This explains the heterogeneity of lattice parameters and their rates of change. The non-uniformity of lattice parameters among the grains means a non-uniformity of lattice expansions, which can be accommodated by sliding or rotation with respect to each other, causing a change in the angle of diffraction. The sliding of groups of grains can create protruberances at the surface.

A grain-dependent heterogeneity of response to interstitial solute input was also found in iron films (114) with hydrogen and in austenitic stainless steel (115). Cathodic charging of hydrogen into pure iron, low-carbon iron, and commercial steels causes dislocation tangles at grain boundaries and inclusion interfaces, as well as microvoids and microcracks (116-118). Raczynski (119) found that cathodic charging of extremely pure iron does not produce dislocations or internal voids. Beck et al. (120) found that

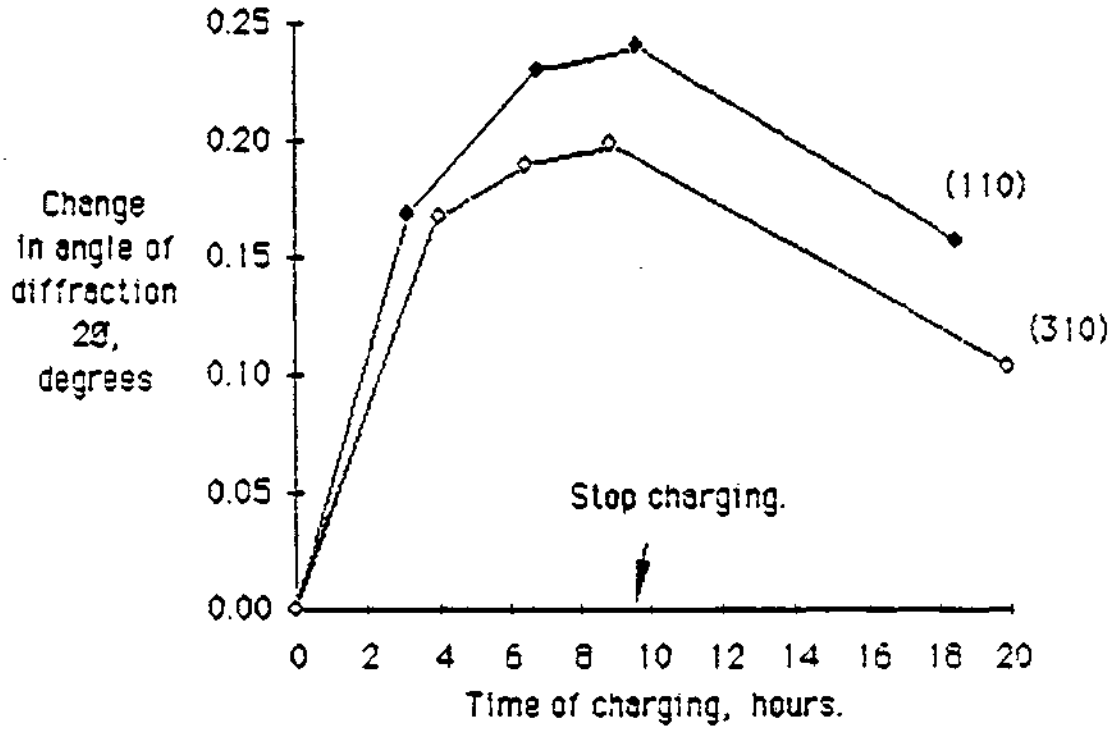

Figure 6. Rotation of crystal grains at the far side of a Ti-30 Mo plate caused by cathodic charging of hydrogen at the other side (Ref. 111).

nominally pure iron exhibits a threshold input fugacity for the production of internal defects, as observed by permeation transients. Charging in of hydrogen produced by low-pressure plasma was found (121) to produce dislocations in Monel and in 304 stainless steel even at depths beyond the penetration depth of the hydrogen ions.

The foregoing discussion deals with phenomena associated with coherency stresses produced by the lattice expansion stresses caused by the lattice expansion associated with lattice-dissolved hydrogen. If in addition second phases are formed as the hydrogen moves in, even greater motivation for dislocation generation results because of the large and abrupt volume change. For example, the precipitation of ε or β phase from Nb-H solid solution produces irregularly shaped particles which emit prismatic dislocation loops which persist even after the two-phase alloy is warmed into the one-phase field (122). Similar results were seen by Lecoq (123) with the formation of β phase in α-$TaH_{0.1}$; the β phase was found to be surrounded by dense dislocation tangles. For Pd, Wise et al. (124) found large dislocation densities in metal in which the β phase had formed and had subsequently decomposed. Jamieson et al. (61) observed that the disappearance of β phase, caused by allowing hydrogen to evolve from the Pd-H alloy, is accompanied by dislocation generation. Storms and Talcott-Storms (125) found a high dislocation density in a Pd sample that had been repeatedly cycled between low and high hydrogen content. Large dislocation density was seen by Guruswamy et al. (126) in a Pd electrode charged cathodically with deuterium. The plastic deformation was evidenced also by the increase of the electrical resistance by a factor of two and by Doppler line broadening of the electron-positron annihilation peak at 512 keV. Fewer dislocations are produced in palladium if hydrogen charging is carried out so that phase separation is avoided (127). Because the so-called α and β phases of the Pd-H system are really one phase into which a miscibility gap intrudes, abrupt volume changes can be avoided by adjusting hydrogen gas pressure and temperature to surmount the critical point of the miscibility gap.

Changes of Shape. That charging hydrogen into a metal can change the shape of the specimen is common knowledge. Smialowski (117) measured the expansion of the diameters of cylindrical specimens of low- and medium-carbon steels. He found that the dilation occurred only above an ill-defined threshold value of f_i, and that the relative expansion increased with decreasing specimen radius. Krause and Kahlenberg (115) found that cycling palladium between absorption and evolution of hydrogen increases the thickness and decreases the other dimensions of a specimen. Storms and Talcott-Storms (125) found that cycling Pd between a hydrogen concentration above the minimum concentration of the β phase and a low concentration thickens a disc-shaped specimen and decreases its diameter (as measured after extraction of hydrogen), and similar treatment of a rod of Pd increased the diameter and decreased the length. The change of the dimensions was accompanied by an increase of overall volume which was larger as the number of cycles was increased. In addition, large populations of microvoids were observed on polished cross-sections of the specimens after cycling. These authors inferred that the observed microvoids are the intersection of tubules, or channels, within the metal with the surface of observation. Matsumoto (128) observed, in Pd cathodically charged to an unspecified level of hydrogen or deuterium

concentration, "tiny spots" often arranged along grain boundaries. These features have all the characteristics of microvoids (Fig. 6); these, in other locations have linked together to form crevices. These crevices in some cases grow together to completely surround a metal grain; metallographic preparation apparently causes some of these "excavated" grains to fall out leaving a grain-shaped cavity. In addition, linear cracks are observed (Fig. 7) which in some cases appear to have formed by a linking up of the crevices at grain boundaries. Matsumoto (128) appears inclined to attribute these features to effects of cold fusion that are asserted to have been produced in all of the Pd specimens examined whether charged with deuterium or with hydrogen. Unfortunately, microstructural observations were not made on Pd electrodes that gave no reason to suspect the development of cold fusion. An extreme case of cracking and fissuring caused by deuterium charging is shown in Fig. 8. The 1/8-inch diameter Pd rod was the anode in a fused salt electrolyte in an attempt (129) to replicate Liaw et al.'s (96) high-temperature electrolysis.

It will be recognized that the microstructural phenomena observed in palladium after hydrogen charging have much in common with what happens in hydrogen-charged steels, a field which has been studied extensively (130). With steels, an increase of the diameter of a thin rod or of the thickness of a thin disk is usually associated with the formation and enlargement of microvoids and microcracks caused by the huge gas pressures developed in these internal spaces by recombination of the dissolved hydrogen which is at extremely high thermodynamic activity owing to the very large f_i of the cathodic charging process. The internal cavities expand in the direction of the smallest dimension of the specimen since that involves smallest resistance to plastic flow. The microvoids are preferentially nucleated at grain boundaries, and internal interfaces, especially at those having segregated impurities. It is also well known that the internally pressurized voids develop lenticular shapes and that they link together to produce cracks (131). The phenomena observed by Matsumoto have similar characteristics. The second-phase interfaces that help to nucleate microvoids may be at β-phase particles as well as at grain boundaries, the nucleation being produced by stress developed by dislocation pile-ups. However, this mechanism can operate in Pd only when f_i is so large that the corresponding pressure of the recombined gas within microcavities is large enough to overcome the flow stress in the metal. Extrapolation of the isotherms of Fig. 3.4 of ref. 6 shows that at H/Pd ≈0.9 at 20°C, $p_{H_2} \approx 10^3$ atm, so that the internal pressurization mechanism is not a probable one.

In steels voids form readily by interfacial decohesion around inclusions, by the cracking of second-phase particles, and by the operation of high stresses produced by plastic incompatibility in regions between particles. In hydrogen-charged palladium the second-phase particles are the β-phase nuclei growing in the α-matrix, and plastic flow is caused by the coherence stresses developed by the concentration gradient of the incoming hydrogen, as well as by the volume disparity between the β and the α-phases (calculated for an equal number of Pd atoms). Because the flow stress of the β-phase is larger than that of the surrounding α-phase (132), the disparity in plastic strain across the interface develops large stresses (133) tending to rupture the interface already weakened by impurities and by hydrogen (134). The microvoids thus nucleated grow

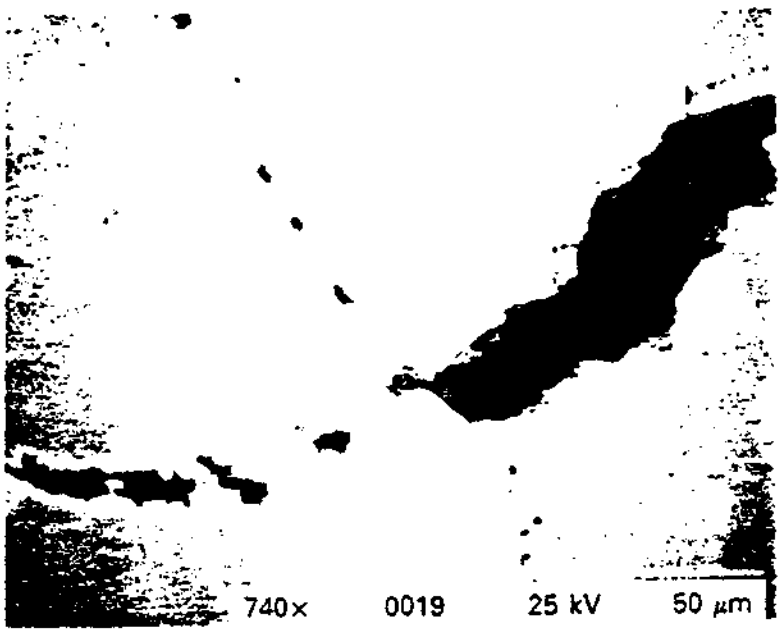

Figure 7. Cavities formed at grain boundaries in palladium by cathodic charging of hydrogen (Ref. 128).

Figure 8. Palladium rod after anodic charging with deuterium by high-temperature electrolysis in molten salt (Ref. 129).

in size by plastic mechanisms, and the growth causes the overall dimensions of the specimen to increase, the smaller dimension increasing more than the larger dimension. At the stage of charging when only β phase is present, compatibility stresses continue to exist because the amount of plastic deformation of any one β-grain depends on its orientation, as observed for Ti-30 Mo (111).

This mechanism does not explain the shrinkage of the length of a Pd rod and of the diameter of a disk (125). It is suggested that these effects result from the preferential direction of motion parallel to the diffusive flux of hydrogen of dislocations impelled by the coherency stresses generated by the hydrogen concentration gradient during charging. Effectively, mass is moved by the dislocations so as to shrink the diameter of the disk and increase its thickness. Cracks are formed in the palladium by the coalescence of closely spaced microvoids, the coalescence being caused by the development of plastic instability in the metal between the voids (135). Another probable mechanism is the localized slip that is known (136) to cause the advance of cracks in several metals. It the space opened up by decohesion at an interface has a lenticular shape with a sharp perimeter and if it is properly oriented with respect to the local stress, the microcrack can advance by hydrogen-aided emission (136) of edge dislocations or by decohesion (137).

Changes of Surface Structure. Rolison et al. (138) carefully studied the variety of surface morphologies produced on the input surfaces of palladium by cathodic charging with hydrogen and with deterium. The polycrystalline foil employed was first etched, producing a variety of micromorphologies; which morphology develops with etching presumably depends on the crystallography of the exposed surface. The long-duration of subsequent cathodic deposition made it impossible to obtain channeling patterns, good evidence for extensive plastic deformation. The micromorphology of the grain surfaces was changed, in different ways for different grain surfaces, by the cathodic charging. The changes are related to the plastic deformation of the grains, and the differences among the grains arise from the differences in the stresses developed, the rate of hydrogen absorption which depends on the crystallography of the surface, the disposition of slip planes with respect to the free surface, and the amount of plastic deformation produced in any one grain. That different modifications of the various etch-produced morphologies result from the cathodic charging is not surprising since the plastic response depends on many factors that very from grain to grain. Modification of the surface morphology by hydrogen charging into Ti-30 Mo alloy (111, 139) was discussed in a previous section; variations of surface morphology were observed but not specifically studied.

What is more surprising is the difference found (138) for the surface morphologies generated by hydrogen and by deuterium charging. Deuterium charging produced a morphology different from that produced by hydrogen, starting from the same type of etch-produced surface. In addition, deuterium charging caused some grains to protrude slightly beyond the plane of the surrounding grain surfaces. This effect was not seen with hydrogen charging. Several reasons for differences between hydrogen charging and deuterium charging may be cited: the difference in partial molal volume

producing a difference in the gradient-caused coherence stress, the presumed difference in the interaction with dislocation cores, and perhaps most important, the difference in f_i of cathodic charging despite the sameness of the imposed electrical charging current for both isotopes. This sameness does not insure identical f_i-time history because of the different ionic conductivities of the H_2O-Li_2SO_4 and D_2O-Li_2SO_4 electrolytes, and the presumed difference of atom recombination on the Pd surface. Very careful investigation will be needed to understand the difference between the two isotopes with respect to grain relief. However, that uplift can occur is not too surprising since protruberances were seen also in the cathodic charging of Ti-30 Mo (111).

Effects of Hydrogen on Mechanical Properties

Both the phenomenology of, and the attempts to understand, the effects of dissolved hydrogen on the mechanical responses of metals are very large subjects. This review can only briefly touch on the salient points.

The paramount and ubiquitous effect of hydrogen on mechanical properties is embrittlement. This means that with some hydrogen in the metal, less work is needed to cause mechanical failure for a given load-time history. This decrease may be manifested by a decrease in the tensile elongation (strain) to cause failure, by the decrease of static load that can be sustained by the metal, by a decrease of the number of load-no load cycles, or by an increase of the rate of crack propagation. It is important to recognize that the effects of hydrogen depend in complex and mutually interacting ways on purity level, impurity distribution, microstructure and phase distribution, prior mechanical history (e.g., extent and kind of deformation), surface chemistry and geometry (e.g., notches), etc., for a given alloy composition. For some metals a fraction of a part per million hydrogen content (e.g., in high -strength steels) is sufficient to develop catastrophic embrittlement (118). For others (e.g., Nb, Ta) sufficient hydrogen concentrations to sustain hydride formation is required for serious embrittlement.

This review can discuss the mechanism for the effects of hydrogen only very superficially. The most important factor is the ability of dissolved hydrogen to lessen the binding forces between metal atoms; this is discussed in a previous section of this review. This effect can manifest itself by a reduction of the force for the normal (i.e., co-linear) separation of two portions of a body, leading to the easier propagation of a cleavage crack (140), or by reduction of the force needed for the continuous emission of edge dislocations from the tip of a crack (141) leading to easier crack propagation by localized plasticity. Which of these occurs, or what mix of these modes takes place in any one instance depends on many factors. These problems have been intensively studied in materials of construction, but very little in palladium and its alloys.

Hydrogen at low concentrations in pure nickel, α-iron, α-titanium and niobium decreases the flow stress (142). At tips of cracks in bodies under externally applied tensile forces, the hydrogen concentrates and causes localized plasticity which produces an easier crack propagation. Impurities change the response drastically. Large concentrations of hydrogen in Ti, Ta, V and Nb produce brittleness because the

hydrides that are formed resist dislocation motion. In palladium (132) hydrogen increases the mechanical hardness. At low concentrations the flow stress is increased but, amazingly, the elongation at fracture is also, increased (132). This behavior may vary with impurity content, which was not explored by Hasegawa and Nakajima (132); it may explain the finding (125) that cycling the hydrogen content totally within the (α+β) field of palladium-hydrogen does not generate excess volume, that is, internal voids and fissures do not develop because plastic deformation of the α-phase remains easy. However, at high hydrogen concentrations such that only the β-phase is present, the elongation at fracture is much reduced because the mobility of dislocations is decreased. Thus, the cathodic charging of palladium, or of any metal, generates mechanical stresses through the kinetics of hydrogen input, and the hydrogen content modifies the responses of the metal to the mechanical stress. The dynamics of these processes deserve much more study than they have received.

Implications for Cold Fusion Research

A popular idea in the field of cold fusion research is that a large D/M ratio is a pre-requisite for the generation of the so-called excess power (143). To obtain a large loading ratio it is necessary to facilitate the entry of hydrogen from the ad-layer and to impede the recombination of hydrogen atoms that transit from the sub-surface layer to the ad-layer. Because the kinetics of transit into the metal and of recombination are each strong functions of the atomic arrangements of metal atoms on the surface one must expect that there will be differences in the rate of loading from one crystal grain to another depending on the nature of the surface that the grain presents to the environment. These differences can be large during charging. Under steady-state conditions small differences between grains in average hydrogen concentration should persist. It will be difficult to maintain a desirable surface configuration (i.e., one that facilitates input and impedes egress) because the surface topography is changed during charging by dislocation activity, as well as by the deposition of impurities.

Patches of surface characterized by low values of f_i will serve as leaks for high-concentration regions under adjoining patches of high-f_i surface. Thus, diffusion currents of dissolved hydrogen can be established between surface patches even at steady-state conditions. Other leaks for hydrogen would be, in some circumstances, grain boundaries and dislocations that terminate at the free surface. The role of microcracks as hydrogen leaks has been emphasized by Storms (125), if these communicate with the surface. If the microcracks or voids are totally within the volume of the metal, they will have only a transient effect on the local hydrogen concentration.

One of the views (144) as to the mechanism of cold fusion involves the periodic potential that would be provided by stoichiometric PdD. This mechanism must deal with the thermodynamic necessity that an interstitial solute cannot completely occupy one class of sites, as discussed in an earlier section. As D/Pd approaches one, some octahedral sites must remain empty with the additional D atoms going into tetrahedral sites of higher energy. What this does to the quantum mechanical picture (144) should

be considered. Incidentally, it can be expected that the deuterium atoms in tetrahedral sites will have a larger mobility than those in the lower-lying octahedral sites. Furthermore, if spatially large domains of near-perfect order are contemplated by this model (144), it would be highly desirable to avoid dislocation generation by slow charging in of hydrogen in such a way that the $\alpha+\beta$ phase field is avoided, or by the use of superlattice alloys that do not have a two-phase field of hydrogen solutions.

In considering various possibilities by which cold fusion may be thought to take place it will be helpful to realize that high input fugacity sources, used to produce large D/M ratios, do not generate pressure to push or squeeze dissolved deuterium atoms together, or into close proximity. In fact the lattice sites are expanded. Another idea that needs reconsideration is that of fractofusion (145), whereby the quickly separating crack surfaces become oppositely charged and the ensuing electric field accelerates deuterons the collision of which results in fusion. Leaving aside many questions that may be asked about this model, only the speed of separation of the crack surfaces will be mentioned here. If hydrogen-aided localized plasticity is the mechanism of cracking of palladium it is implausible that the created free surfaces will separate so rapidly that electrons will not have time to move to neutralize the putative charge on the crack surfaces.

The generation of dislocations by hydrogen charging makes another argument implausible. This is the argument that the excess heat that some investigators of cold fusion report is really the release of stored energy such a mechanical energy of the stresses in the metal. The problem with this idea is that the energy of the stress field, proportional to σ^2/E, is continually degraded into heat by the continuous generation and motion of dislocations and cracks. At the stress levels involved the multiplication of dislocations is easy, so that the mechanical energy cannot attain larger magnitudes. Furthermore, the conversion of the energy stored in the dislocations cannot be easily converted into heat, as shown by Shober (122) who found that raising the temperature was not effective in causing the disappearance of dislocations formed by the re-dissolution of ε-NbH_x.

References

1. "Hydrogen in Metals," G. Alefeld and J. Volkl, eds., Springer-Verlag, Berlin, Vols. 1 and 2, 1978.

2. "Metals-Hydrogen Systems," R. Kirchheim, E. Fromm, E. Wicke, R. Oldenbourg Verlag, Munchen, 1989.

3. E. Wicke and G.H. Nernst, Ber Bunsenges. Phys. Chem. 68, 224 (1964).

4. S. Schmidt, Diplomarbeti, Munster (1978).

5. J.D. Clewley, T. Curran, T.B. Flanagan and W.A. Oates, J. Chem. Soc. Faraday Trans. 169, 449 (1973).

6. G. Sicking, Z. Physik. Chem. (N.F.) 93, 53 (1974).

7. G. Sicking, Ber Bunsenges. Physik. Chem. 76, 790 (1972).

8. E. Wicke and H. Brodowsky, in Ref. 1, Vol. II, p. 73.

9. H. Brodowsky, H. Gibmeyer and E. Wicke, Z. Physik. Chem. (N.F.) 49, 222 (1966).

10. E. Storms and C.Talcott-Storms, Fusion Techn. 20, 246 (1991).

11. J.F. Lynch and T.B. Flanagan, J. Phys. Chem. 77, 2628 (1973).

12. U. Stolz, U. Nagorny and R. Kirchheim, Scripta Metall. 18, 347 (1984).

13. H. Peisl, in Ref. 1, Vol. I, p.53.

14. W.T. Lindsay Jr., Abstracts of ACS National Meeting, Pittsburgh, March 1966.

15. A.J. Maeland and T.B. Flanagan, J. Phys. Chem. 18, 1419 (1964).

16. R. Abbenseth and H. Wipf, J. Phys. E. Metal Phys. 10, 353 (1980); J.E. Shirber and B. Morosin, Phys. Rev. B 12, 117 (1975).

17. H.A. Wriedt and R.A. Oriani, Acta Metall. 18, 753 (1970), from data by W.T. Lindsay Jr.

18. T. Schober and H. Wenzel in Ref. 1, Vol II, p.11.

19. D.T. Peterson and H.M. Herro (Dept. Mater. Sci. Iowa State University, Ames), Abstracts of The Metallurgical Society.

20. R.A. Oriani, Trans. Metall. Soc. AIME, 236, 1368 (1966).

21. H. Wagenblast and H.A. Wriedt, Metall. Trans. 2, 1393 (1971).

22. R.A. Oriani, Proc. Conf. Fundamental Aspects of SCC, Columbus 1967, N.A.C.E., R.W. Staehle, A.J. Forty and D. Van Rooyen, eds., pp. 32-50 (1968).

23. A.D. McQuillan, C.E. Ellis, H. Pessal, A.P. Bennett, J. Basterfield and A.D. Wallbank: "The Solution of Hydrogen in B.C.C. Metals," Report from the University of Birmingham, 1964.

24. R.E. Rundle, C.G. Shull and E.O. Wollan, Acta Cryst. 5, 22 (1952).

25. J.L. Waisman, G. Sents and L.B. Robinson, Metall. Trans. 4, 291 (1973).

26. E.O. Wollan, J.W. Cable and W.C. Koehler, J. Phys. Chem. Solids 24, 1141 (1963).

27. B. Baranowski, S. Majehrzak and T.B. Flanagan, J. Phys. F: Metal Phys. 1, 258 (1971).

28. M. Krukowski and B. Baranowski, J. Less-Common Metals, 49, 385 (1976).

29. K. Heindlhofer, presented in "Physical Chemistry of Metals," L.S. Darken and R.W. Gurry, McGraw-Hill, 1953.

30. V.A. Somenkov, I.R. Entin, A.Y. Chervyakov, S. Sh. Shil'stein and A.A. Chertkov, Sov. Pys. Solid State 13, 2178 (1972).

31. A.Y. Chervyakov, I.R. Entin, V.A. Somenkov, S. Sh. Shil'stein and A.A. Chertkov, Sov. Phys. Solid State 13, 2172 (1972).

32. V.A. Semenkov, A.V. Gurskaya, M.G. Semlyanov, M.E. Kost, N.A. Chernoplekov, and A.A. Chertkov, Sov. Phys. Solid State 10, 2123 (1969).

33. V.F. Petrunin, V.A. Somenkov, S. Sh. Shil'stein, A.A. Chertkov, Sov. Phys. Cristallography 15, 137 (1970).

34. H.G. Fritsche, H. Muller and Ch. Optiz, in Rf. 2, p. 535.

35. J. Friedel, Ber. Bunsenges, Physik. Chem. 76, 828 (1972).

36. J.C. Fisher, Acta Metall. 6, 13 (1958).

37. G.J. Zimmerman, J. Less-Common Metals 49, 49 (1976).

38. W. Drexel, A. Murani, D. Tocchetti, W. Kley, I. Sosnowska, and D.K. Ross, J. Phys. Chem. Sol. 37 1135 (1976).

39. W. Zhong, Y. Cai, and D. Tomanek, Phys. Rev. B, 46, 8099 (1992).

40. R.P. Messmer and C.L. Briant, Acta Metall. 30, 457 (1982).

41. M.S. Daw and M.I. Baskes, Phys. Rev. B, 29, 6443 (1984).

42. T. McMullen, M.J. Stott and E. Zaremba, Phys. Rev. B, 35, 1076 (1987).

43. H.G. Fritsche and H.G. Muller, Z. Phys. Chem. (Leipzig), 266, 595 (1985).

44. R. Kirchheim, Acta Metall. 34, 37 (1986).

45. C. Budin, A. Lucasson, and P. Lucasson, J. Phys. (Paris) 25, 751 (1964).

46. G.R. Caskey Jr., R.G. Derrick, Scripta Metall. 10, 377 (1976).

47. J.P. Hirth, Metall. Trans. A, 11A, 861 (1980).

48. A.J. Kummick and H.H. Johnson, Acta Metall. 28, 33 (1980).

49. H.H. Podgurski and R.A. Oriani, Metall. Trans. 3, 2055 (1972).

50. R. Kirchheim, Acta Metall. 29, 835, 845 (1981).

51. G.J. Thomas, in "Hydrogen Effects in Metals," Met. Soc. AIME (1981), I.M. Bernstein and A.W. Thompson, eds., p. 77.

52. T. Mutschele and R. Kirchheim, Scripta Metall. 21, 135 (1987).

53. S.W. Stafford and R.B. McLellan, Acta Metall. 22, 1463 (1974).

54. H. Ohma, G.P. Tivari, Y. Iijima and K. Hirano, Proc. 2nd J.I.M. Intnl. Symp. "Hydrogen in Metals" (1979), Jap. Inst. Metals, p. 229.

55. M.B. Whiteman and A.R. Troiano, Phys. Status Solids, 7, K109 (1964).

56. J.P. Laurent, G. Lapasset, G. Aucouturier, and M. Lacombe, in "Hydrogen in Metals," Met. Soc. AIME (1974), I.M. Bernstein and A.W. Thompson, eds., p. 559.

57. J.C.M. Li, R.A. Oriani, and L.S. Darken, Z. Physik Chem. (N.F.) 49, 271 (1966).

58. R.A. Oriani, Acta Metall. 14, 84 (1966).

59. H. Frieske and E. Wicke, Ber. Bunsenges, Physik. Chem. 77, 50 (1973).

60. H. Wagner, in Ref. 1, Vol. 1, p. 5.

61. H.C. Jamieson, G.C. Weatherly, and F.D. Manchester, J. Less-Common Metals 50, 85 (1976).

62. K.W. Keher, in Ref. 1, Vol. I, p. 197.

63. J. Volkl and G. Alefeld, in Ref. 1, Vol. I, p. 321.

64. J. Volkl, G. Wollenweber, K.H. Klatt and G. Alefeld, Naturforsch 26A, 922 (1971).

65. H.G. Nelson and J.E. Stein, NASA Report TND-7265 (1973).

66. Ref. 22, calculated from O.D. Gonzalez, Trans. Metall. Soc. AIME 245, 607 (1969).

67. Y. Hayashi, H. Hagi and A. Tahara, in Ref. 2, p. 815.

68. B. Baranowski, in Ref. 1, Vol. II, p. 157.

69. R. Gomer, R. Wortman and R. Lundy, J. Chem. Phys. 26, 1147 (1957).

70. R. Wortman, R. Gomer, and R. Lundy, J. Chem. Phys. 27, 1099 (1957).

71. M.L. Hill and E.W. Johnson, Acta Metall. 3, 566 (1955).

72. D.R. Arantes, X.Y. Huang, C. Marte and R. Kirchheim, Acta Metall. 41, 3215 (1993).

73. T.M. Harris, and R.M. Latanision Metall. Trans A, 22A, 351 (1991).

74. E.G. Seebauer, A.C.F. Kong, and L.D. Schmidt, J. Chem. Phys. 88, 6597 (1988).

75. L.S. Darken and R.P. Smith, Corrosion 5, 1 (1949).

76. T. Matsumoto, J. Phys. Soc. Japan, 42, 1583 (1977).

77. C.A. Wert, in Ref. 1, Vol. II, p. 305.

78. O. Yoshinari, K. Suito, T. Miura, and K. Tanaka, in Ref. 2, p. 825.

79. C.G. Chen and H.K. Birnbaum, Phys. Status Solids 36a 687 (1976).

80. G.M. Pressouyre and I.M. Bernstein, Metall. Trans. A, 9A 571 (1978).

81. A.M. Nabb and P.K. Foster, Trans. Metall. Soc. AIME, 227, 618 (1963).

82. R.A. Oriani, Acta Metall. 18, 147 (1970).

83. R. Kirchheim, Scripta Metall. 14, 905 (1980).

84. P. Bastien and P. Azou, Compt. Rend. Acad. Sci. Paris, 232, 1845 (1951).

85. M.R. Louthan, G.R. Caskey, J.A. Donovan and D.W. Rawl, Mater. Sci. Eng. 10, 357 (1972).

86. M.R. Louthan, pp. 53-78 "Hydrogen in Metals," I.M. Bernstein and A.W. Thompson, eds. ASM, Metals Park, OH, 1974.

87. K.G. Denbigh, "The Thermodynamics of the Steady State," Methuen, London (1951).

88. H. Wipf, in Ref. 1, Vol. II, p. 273.

89. R.A. Oriani and O.D. Gonzalez, Trans. Met. Soc. AIME 239, 1041 (1967).

90. O.D. Gonzalez and R.A. Oriani, Trans. Met. Soc. AIME 233, 1878 (1965).

91. A.W. Aldag and L.D. Schmidt, J. Catalysis 22, 260 (1971).

92. H. Conrad, G. Ertl, and E.E. Latta, Surface Sci. 41, 435 (1974).

93. W.H. Weinberg and R.P. Merrill, Surface Sci. 33, 493 (1972).

94. W. Aver and H.J. Grabke, Ber. Bunsenges. Physik. Chem. 78, 58 (1974).

95. W. Palczewska, Bull. Acad. Polon. Sci., Ser. Sci. Chim. 12, 817 (1964).

96. B.Y. Liaw, P.-L. Tao, P. Turner, B.E. Liebert, J. Electronal, Chem. 319, 161 (1991).

97. Stackelberg and Bischoff, Z. Elektrochem. 58, 702 (1955).

98. E. Storms, C. Talcott and M.L. David, Proc. NSF-EPRI Workshop on Anomalous Effects in Deuterated Metlas, Washington 1989; p. 5-1.

99. J.F. Newman and L.L. Shreir, Corros. Sci. 9, 631 (1969).

100. T. Zakroczymski, Z. Szklarska-Smialowska and M. Smialowski, Werkst. Korros. 26, 624 (1975).

101. A.M. Riley, J.D. Seader, D.W. Pershing, A. Linton, and S. Shimizu, Report NCFI-3, National Cold Fusion Institute, Utah 1990.

102. A. Efron, Y. Lifshitz, I. Lewkowicz, in Ref. 2, p. 1255.

103. B.Baranowski, Ber. Bunsenges. Physik. 76, 714 (1972).

104. R.A. Oriani and P.H. Josephic, Proc. Symp. "Environment Sensitive Fracture of Engineering Materials," Met. So. AIME, Z.A. Foroulis, ed., (1979) pp. 440-450; R.A. Oriani, Proc. "Hydrogen Effects in Metals," I.M. Bernstein, A.W. Thompson, eds., Met. Soc. AIME 1981, pp. 235-54.

105. E. Riecke, Werkst. Korros. 29, 106 (1978).

106. G.H. Schwuttke and H.J. Queisser, J. Appl. Phys. 33 1540 (1962).

107. D.P. Miller, J.E. Moore, and C.R. Moore, J. Appl. Phys. 33, 2648 (1962).

108. J. Washburn, G. Thomas and H.J. Queisser, J. Appl. Phys. 35, 1909 (1964).

109. S. Prussin, J. Appl. Phys. 32, 1876 (1961).

110. J.C.M. Li, Metall. Trans. A, 9A, 1353 (1978).

111. M.E. Armacanqui and R.A. Oriani, Mater. Sci. Eng. 91, 143 (1987).

112. J.K. Boah and P.G. Winchell, Metall. Trans. A, 6A, 717 (1975).

113. T. Sakuma, S. Takada, M. Hasabe and T. Nishizawa Trans. Japan Inst. Met. 17, 637 (1976).

114. M.E. Armacanqui and R.A. Oriani, Mater. Sci. Eng. 92, 127 (1987).

115. W. Krause and L. Kahlenberg, Trans. Electrochem. Soc. 68, 449 (1935).

116. T. Takeyama and H. Takahashi, Proc. 2nd J.I.M. Intnl. Symp. "Hydrogen in Metals" (1979), Japan Inst. Metals p. 409.

117. M. Smialowski, Scripta Metall. 13, 393 (1979).

118. C.P. Ju, J. Don and J.M. Rigsbee, Mater. Sci. Eng. 77, 115 (1986).

119. W. Raczynski, personal communication from M. Smialowski, 1975.

120. W. Beck, J. O'M. Bockris, J. McBreen and L. Nanis, Proc. Roy. Soc. (London) A290, 220 (1966).

121. S. Veprek, F. Mattenberger, M. Heintze, M. Wiggins, M. Kitajima, K. Yamashita, and R. Gotthardt, J. Vac. Sci. Techn. A7, 69 (1989).

122. T. Schober, Scripta Metall. 7 1119 (1973).

123. P. Lecoq, Ph.D. thesis, University of Illinois 1974.

124. M. Wise, J. Farr, I. Harris and J. Hirst, in "L'Hydrogene dans les Metaux," Vol. 1, p. 1, Editions Schience et Industrie, Paris 1972.

125. E. Storms and C. Talcott-Storms, Fusion Techn. 20, 246 (1991).

126. S. Guruswamy, J.G. Byrne, J. Li and M.E. Wadsworth, Proc. EPRI-NSF Workshop on Anomalous Effects in Deuterated Metals, Washington, D.C., (1989) p. 16-1.

127. T.B. Flanagan, ibid., p. 4-1.

128. T. Matsumoto Fusion Techn. 19, 567 (1991).

129. R.A. Oriani, unpublished results.

130. "Hydrogen Degradation of Ferrous Alloys," R.A. Oriani, J.P. Hirth and M. Smialowshi, eds., Noyes Publications Park Ridge, NJ, 1985.

131. M. Iino, in Ref. 130, p. 737.

132. H. Hasegawa and K. Nakajima, Phys. F. Metal. Phys. 9, 1035 (1979).

133. L.M. Brown and J.D. Embury, Proc., The Institute of Metals, Vol. 1, p. 164 (1973); W. Roberts, B. Lehtinen and K.E. Easterling, Acta Metall. 24, 745 (1976).

134. K. Yoshiino and C.J. McMahon Jr., Metall. Trans. 5, 363 (1974).

135. O.A. Onyewuenyi, in Ref. 128, p. 414.

136. T. Tabata and h.K. Birnbaum, Scripta Metall. 17, 947 (1983); 18, 231 (1984).

137. R.A. Oriani, Corrosion 43, 390 (1987).

138. D.R. Rolison and P.P. Trzaskoma, J. Electroanal. Chem. 287, 375 (1990); P.P. Trzaskoma, D.R. Rolison and R.G. Vardiman, in Proc. "Application of Surface Analysis Methods to Environmental Materials Interactions," Electrochemical Society meeting Oct. 1990, Seattle.

139. M.E. Armacanqui and R.A. Oriani, Mater. Sci. Eng. 92, 127 (1987).

140. R.A. Oriani, Ann. Rev. Mater. Sci. 8, 327 (1978).

141. C.D. Beachem, Metall. Trans. 3, 437 (1972); S.P. Lynch, Scripta Metall. 13, 1051 (1979).

142. H.K. Birnbaum, Proc. 1st Intnl. Conf. "Environment-Induced Cracking of Metals," R.P. Gangloff, M.B. Iver, eds., NACE, 1990, pp. 21-30.

143. M.C.H. McKubre, S. Crouch-Baker, A.M. Riley, S.I. Smedley, and F.L. Tanzella, Proc. 3rd Intnl. Conf. Cold Fusion 1992.

144. T.A. Chubb and S.R. Chubb, Fusion Techn. 17, 710 (1990).

145. P.I. Golubnicki, V.A. Kurakin, A.D. Filonenko et. al., Dokl. Akad. Nauk. SSSR 307, 99 (1989). [Sov. Phys. Dokl. 34 (7) 628 (1989).

Table I. Partial Molal Volume of H and of D in Various Metals

Host Metal	$\bar{V}_H$ *cm³ mol⁻¹*	*Reference*	$\bar{V}_H/\bar{V}_D$	*Reference*	*Site Occupied**	*Reference*
Pd	1.50	12	< 1	15	O	8
	1.57	8	> 1	16		
	1.68	13				
	1.73	14				
$Pd_{.9}Ag_{.1}$			0.97	13		
$Pd_{.75}Ag_{.25}$	1.90	17				
Ta	1.69	13	1.08	13	T	18
Nb	1.89	13	1.0	13	T	18
	1.57	19	0.88	19		
V	1.61	13	1.0	13	T	18
	1.78	19	0.94	19		
α-Ti	2	25				
β-Ti	1.6	23			T	24
β-ZrH_2	2.7	23			T	24
α-Fe	2.0	20,21			O	22
$NiH_{.6}$	1.85	13			O	26

* O: octahedral site; T: tetrahedral site

Table II. Interaction Enthalpies, kJ/mol H, Between Dissolved Hydrogen and Structural Defects

Metal	*Dislocation Cores*	*Reference*	*Grain Boundaries*	*Reference*	*Interphase Interfaces*	*Reference*
α-Fe	-20 to -30 (screw) -59 (mixed)	47 48	~-6.0	47	-65 (AlN) ~-85(Fe_3C) ~-95 (TiC)	49 47 47
Pd	-60 to -70 (edge)	50	-5.3 (σ=15)*	52		
Ni	-9.6 to -19.2	51	-4.3	53		
Co			-8.0	53		

* σ = width of Gaussian distribution

Table III. Diffusivity of Hydrogen at Low Concentrations and About Room Temperature

Host Metal	*Hydrogen Isotope*	D_o $cm^2 s^{-1}$	E_a $kJ\ mol^{-1}$	*Temp Range, °C*	*Reference*
Pd	H	2.9×10^{-3}	22.2	-50 to 600	63
	H	5.3×10^{-3}	22.8		8
	D	2.7×10^{-3}	20.5		8
	D		19.8		64
	T	7.2×10^{-3}	30.1		8
Ni	H	4.8×10^{-3}	39.4	0 to 358	63
α-Fe	H	7.5×10^{-3}	10.1	0 to 770	65
	H	2.3×10^{-3}	6.66		65
	H	0.78×10^{-3}	7.9		66
	H	3.35×10^{-4}	3.4		67
	D	3.35×10^{-4}	5.0		67
Nb	H	5.0×10^{-4}	10.2	0 to 500	63
	D	5.2×10^{-4}	12.3	-125 to 300	63
	T	4.5×10^{-4}	13.0	-50 to 30	63
Ta	H	4.4×10^{-4}	13.5	-20 to 400	63
	D	4.6×10^{-4}	15.4		63
V	H	3.1×10^{-4}	4.3	-125 to 300	63
	D	3.8×10^{-4}	7.0		63
$Pd_{.8}Ag_{.2}$	H	3.4×10^{-3}	22.4		8
	D	1.6×10^{-3}	19.9		8
	T	5.6×10^{-3}	23.9		8
$Pd_{.8}Ni_{1.2}$	T	3.4×10^{-3}	23.9		8

Table IV. Interaction Enthalpies(kJ/molH) Between Dissolved Hydrogen and Dissolved Impurities

Host Metal	*Impurity*	*Interaction Energy*	*Reference*
Nb	V	-8.7	76
	O	-8.7	77
Ta	N	-5.8	77
V	O	-7.4	78
	Ti	-7.0	78
αFe	C	-3.3	79
	Ti	-26	80

Table V. Effective Charge, Z*, and Heat of Transport, Q*, of Hydrogen in Various Metals (From Ref. 88)

Host Metal	*Hydrogen Isotope*	*Z* (unites of electronic charge)*	*Q*, eV/atomH*
α-Ti	H		+0.23
β-Ti	H	Positive for H and D	+0.027
α-Zr	H	Negative	+0.26
β-Zr	H	Negative for H and D	+0.25 to +0.5
δ-Zr	H		+0.056
V	H	+1.6 to + 1.4	+.017 to 0.087
	D	+1.8 to + 1.5	
Nb	H	+2.6 to +2.4	+0.15 to +0.13
	D	+2.1 to +1.9	+0.13 to 0.11
αFe	H	+0.24 to +0.29	-0.35 to -0.24
	D	+0.42 to +0.43	-0.34 to -0.23
Ni	H	+0.67 to +0.57	-0.065 to -0.009
	D	+0.84 to +0.74	-0.056 to -0.035
Pd	H	+0.4 to +0.55	+0.065
	D	+0.51 to +0.59	
Ag	H	-6.8	
	D	-18	
Ta	H	+0.2 to +0.6	
	D	+0.2 to +0.5	

Note: The ranges of values for Z* and Q* pertain to temperature variations of those parameters.

Table VI. Fugacity - Pressure Relationship for Hydrogen Gas at 25°C (from Ref. 103).

Fugacity, atm	*Pressure, atm*
28.1	27.7
247	217
896	609
1860	987
3060	1315
6880	1955
1.25×10^4	2510
1.13×10^5	5045
1.67×10^6	8990
1.01×10^7	1.20×10^4
1.66×10^8	1.73×10^4
1.22×10^9	2.14×10^4